universität wien

MASTERARBEIT / MASTER'S THESIS

Titel der Masterarbeit / Title of the Master's Thesis

LC-MS Analysis of Oxylipins in Plasma Samples from Patients Undergoing Extracorporeal Photopheresis

verfasst von / submitted by

Dexin Dong BSc

angestrebter akademischer Grad / in partial fulfilment of the requirements for the degree of

Master of Science (MSc)

Wien, 2022 / Vienna 2022

Studienkennzahl lt. Studienblatt / degree programme code as it appears on the student record sheet:	UA 066 863
Studienrichtung lt. Studienblatt / degree programme as it appears on the student record sheet:	Masterstudium Biologische Chemie
Betreut von / Supervisor:	Univ.-Prof. Dr. Christopher Gerner

Acknowledgements

I would like to thank Univ.-Prof. Dr. Christopher Gerner for allowing me to work with his group and write this master's thesis under his supervision. I am also grateful to Gerhard Hagn MSc and Julia Brunmair MSc, who introduced me to the analytical methods and data analysis. This work would also not have been possible without Dipl.-Ing. Dr. Johanna Mader and Peter Frühauf, who provided technical support. The thesis was done with the cooperation of Ass.-Prof. Dr. Verena Paulitschke and Dr. Ara Cho from the Department of Dermatology at the Medical University of Vienna, for which I am thankful. Finally, I would like to thank the other members of the group, Ass.-Prof. Dr. Samuel Matthias Meier-Menches, Dr. Astrid Slany, Dr. Andrea Bileck, Benjamin Neuditschko MSc and Lukas Janker MSc.

Contents

List of Figures

List of Tables

Abbreviations

8-MOP	8-methoxypsoralen
AA	Arachidonic acid
ALA	α-linolenic acid
BHT	Butylated hydroxytoluene
COX	Cyclooxygenase
CTCL	Cutaneous T-cell lymphoma
CV	Coefficient of variation
CYP450	Cytochrome P450
DC	Dendritic cell
DDA	Data-dependent acquisition
DGLA	Dihomo-γ-linolenic acid
DHA	Docosahexaenoic acid
DiHETrE	Dihydroxyeicosatrienoic acid
DiHOME	Dihydroxyoctadecenoic acid
DNA	Deoxyribonucleic acid
DPA	Docosapentaenoic acid
ECP	Extracorporeal photopheresis
EDTA	Ethylenediamine tetraacetic acid
EpETrE	Epoxyeicosatrienoic acid
EPA	Eicosapentaenoic acid
ESI	Electrospray ionisation
HESI	Heated electrospray ionisation
FA	Formic acid
GVHD	Graft-versus-host disease
HDoHE	Hydroxydocosahexaenoic acid
HEPE	Hydroxyeicosapentaenoic acid
HETE	Hydroxyeicosatetraenoic acid
HHTrE	Hydroxyheptadecatrienoic acid
HODE	Hydroxyoctadecadienoic acid
HOTrE	Hydroxyoctadecatrienoic acid
HpETE	Hydroperoxyeicosatetraenoic acid
HpODE	Hydroperoxyoctadecadienoic acid
HPLC	High-performance liquid chromatography
LA	Linoleic acid
LOD	Limit of detection

LOQ	Limit of quantification
LOX	Lipoxygenase
LTA_4	Leukotriene A4
MS	Mass spectrometry
m/z	Mass-to-charge ratio
nAUC	Normalised area under curve
Oxo-ETE	ketoeicosatetraenoic acid
Oxo-ODE	Oxooctadecadienoic acid
PUFA	Polyunsaturated fatty acid
SPE	Solid-phase extraction
SPM	Specialized pro-resolving mediators
TXA_2	Thromboxane A_2
UVA	Ultraviolet-A

1 Introduction

Lipidomics is an important part of the growing field of metabolomics. There are eight categories of lipids, which are fatty acyls, glycerolipids, glycerophospholipids, sphingolipids, sterol lipids, prenol lipids, saccharolipids and polyketides. These lipids fulfill a large number of important functions, such as energy storage, cellular communication and membrane formation. Using lipidomics to investigate changes of the lipid profile and metabolism could provide better detection and understanding of various diseases and health conditions, in particular metabolic and autoimmune diseases [1, 2].

Oxylipins are oxidised metabolites of polyunsaturated fatty acids (PUFAs), and are an important part of the body's immune response. They act as lipid mediators between various cells, and play a vital role during the initiation and resolution of inflammation [8, 6]. In many cancer and autoimmune diseases, a significant difference of the oxylipin profile can be observed in comparison to healthy controls [26, 27, 25].

Extracorporeal photopheresis (ECP) is a clinical treatment for cutaneous T-cell lymphoma and is also being investigated for various autoimmune diseases [49]. During ECP therapy, the buffy coat is extracted from the patient's blood, irradiated with ultraviolet-A (UVA) and returned to the patient. The mechanism behind this therapy is still not well understood. In particular, at the time of the writing very few literature on the effects of ECP therapy on the lipidome could be found. The goal of this master's thesis is to investigate and identify changes in the oxylipin profile by comparing plasma samples obtained before and after ECP therapy. Oxylipins were extracted by solid phase extraction (SPE) from plasma samples of six patients undergoing ECP therapy and analysed via UHPLC-MS/MS. It was found that the levels of some oxylipins were significantly increased in the samples obtained post-therapy compared to pre-therapy.

In addition, as part of the master's thesis, an UHPLC-MS/MS method for the analysis of oxylipins was partially developed and compared with the UHPLC-MS/MS method used for the ECP samples.

1.1 Polyunsaturated Fatty Acids

PUFAs are long-chain fatty acids with multiple double bonds. They can be separated into two groups, ω-3 and ω-6, based on the position of the first double bond from the methyl end of the fatty acid. Some important ω-3 and ω-6 PUFAs are depicted in Figure 1. The C18 fatty acids linoleic acid (LA) and α-linolenic acid (ALA) are considered essential, as the human body lacks the enzymes to synthesise them. Other longer-chain PUFAs can be obtained either from the diet or through elongation and desaturation of LA and ALA [6, 8].

PUFAs are bound at the *sn*-2 position of phospholipids in the cell membrane and may play an important role in maintaining the physical properties and organization of the membrane. Modifications to the PUFA composition in the membrane can lead to changes in the size and composition of lipid rafts, affecting their functions [3, 4].

PUFA composition in the body varies from person to person and the intra-individual variability can also be quite high. This may be dependent on the composition of fatty acids taken up in the diet. It is known from literature that the variability of PUFAs in plasma is higher than in red blood cells, which is expected as red blood cells have a lifespan of around 120 days and thus reflect the long-term uptake of PUFA. [5].

The intake of ω-3 PUFAs has been associated with beneficial health effects, such as a reduction of cardiovascular events, though this is often disputed. Some of the most important ω-3 PUFAs are ALA, eicosapentaenoic acid (EPA), ω-3 docosahexaenoic acid (DHA) and docosapentaenoic acid (DPA). Studies have linked their beneficial properties to interactions with the immune system and anti-inflammatory effects, for which multiple mechanisms have been proposed. One of these mechanisms is the increased synthesis of lipid mediators from ω-3 PUFAs [24].

1.2 Oxylipins

Oxylipins are oxidised metabolites of PUFAs, which are usually short-lived. These fatty acyls can be free or esterified, though only the free forms are assumed to be biologically active. Their composition in the body may be influenced by many factors, such as dietary uptake of PUFAs [6, 8]. Differences in lipid metabolism may also determine the oxylipin composition. The group had previously compared the PUFA and oxylipin profile of people with differing brown adipose tissue depots [9].

Eicosanoids, which are one of the more researched classes of oxylipins, specifically refers to the metabolic products of C20 PUFAs such as arachidonic acid (AA), while those of C18 and C22 are termed octadecanoids and docosanoids respectively. The three groups of oxylipins play an

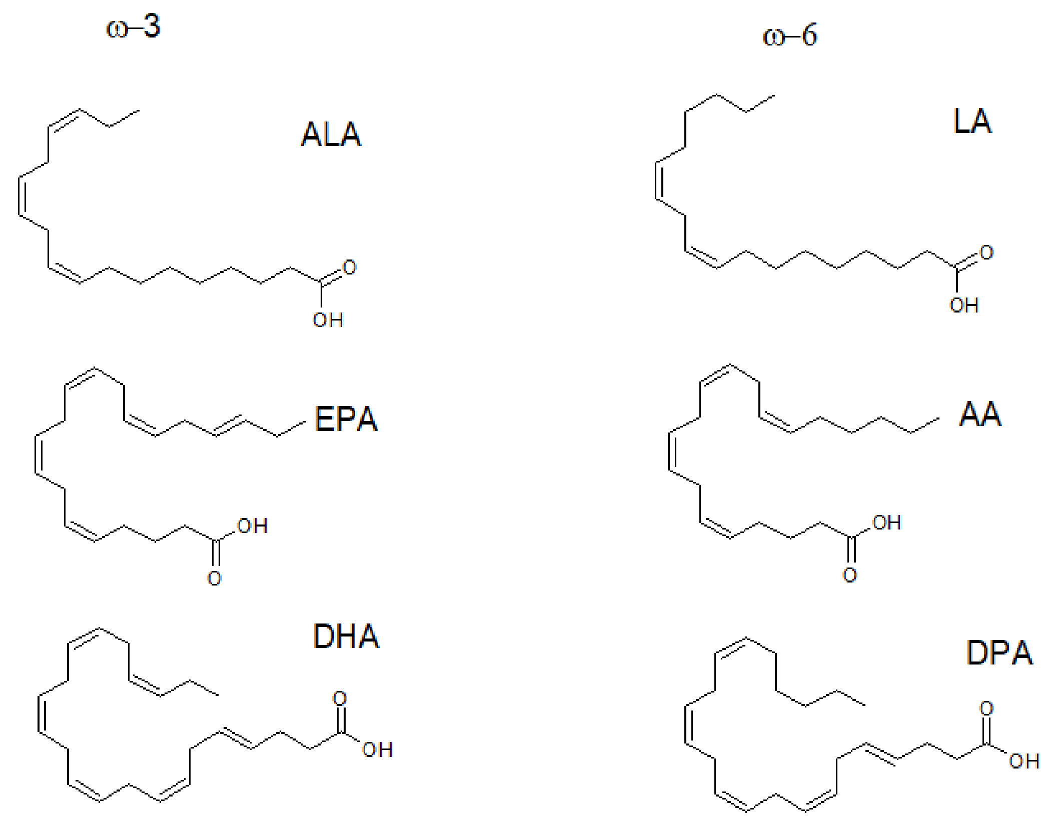

Figure 1: Examples of some polyunsaturated fatty acids (PUFAs). α-linolenic acid (ALA), eicosapentaenoic acid (EPA) and docasahexaenoic acid (DHA) are ω-3 PUFAs, while linoleic acid (LA), arachidonic acid (AA) and ω-6 docosapentaenoic acid (DPA) are ω-6 PUFAs. ω-3 DPA also exists, but is not shown here.

important role as lipid mediators of various functions [6].

In order to metabolise PUFAs, esterified fatty acids at the *sn*-2 position of membrane phospholipids can be released through hydrolysis by phospholipase A2 (PLA_2). This reaction can take place in response to a wide range of possible stimuli, such as through membrane receptors. [6, 7]. There are multiple members of PLA_2, of which cytosolic calcium-dependent PLA_2 ($cPLA_2$) is activated during an inflammatory response. The resulting hydrolysed PUFAs are metabolised into various pro- and anti-inflammatory oxylipins, which regulate the immune response [12].

Oxylipins are generated via three major enzymatic pathways, which are the cyclooxygenase (COX), lipoxygenase (LOX) and cytochrome P450 (CYP450) pathways. The specific product of the pathway is further dependent on other tissue- or cell-dependent enzymes, as well as the local environment [6, 7, 8]. Some examples of possible oxylipin products of AA are shown in Figure 2.

In the COX pathway, the two COX isoforms COX-1 and COX-2 play a role in the generation of prostanoids, which possess a five-carbon ring structure. These can be further metabolised by other enzymes, forming products such as thromboxane A_2 (TXA_2) and prostaglandin E_2 (PGE_2) from PGH_2, an AA product. COX-1 is continuously expressed in most tissues, while COX-2 is usually only expressed during inflammation [6, 7, 8]. In addition, COX-2 is more capable of oxidising some substrates compared to COX-1, such as a number of ω-3 PUFAs [11]. As many products of the COX pathway are involved in inflammation, drugs were developed which specifically targeted these enzymes, in particular the inflammation-activated COX-2. The nonsteroidal anti-inflammatory drugs (NSAID), of which aspirin is the best known, inhibit the COX enzymes, resulting in their anti-inflammatory properties. NSAIDS which also inhibited COX-1 caused undesirable side effects, including gastric ulceration. This resulted in the development of NSAIDs which specifically target COX-2. However, the COX-2 inhibitors were found to have cardiotoxic effects, preventing their clinical use [6, 11].

The LOX pathway results in hydroxy or hydroperoxy products, such as 5-hydroxyeicosatetraenoic acids (HETEs) and 5-hydroperoxyeicosatetraenoic acid (5-HpETE) from AA. The enzymes are named according to the position where the oxygen atom is bonded in AA products, for example 5-LOX. Further metabolism by the LOX enzymes can result in the formation of keto and epoxy products. Some examples are 5-ketoeicosatetraenoic acid (5-Oxo-

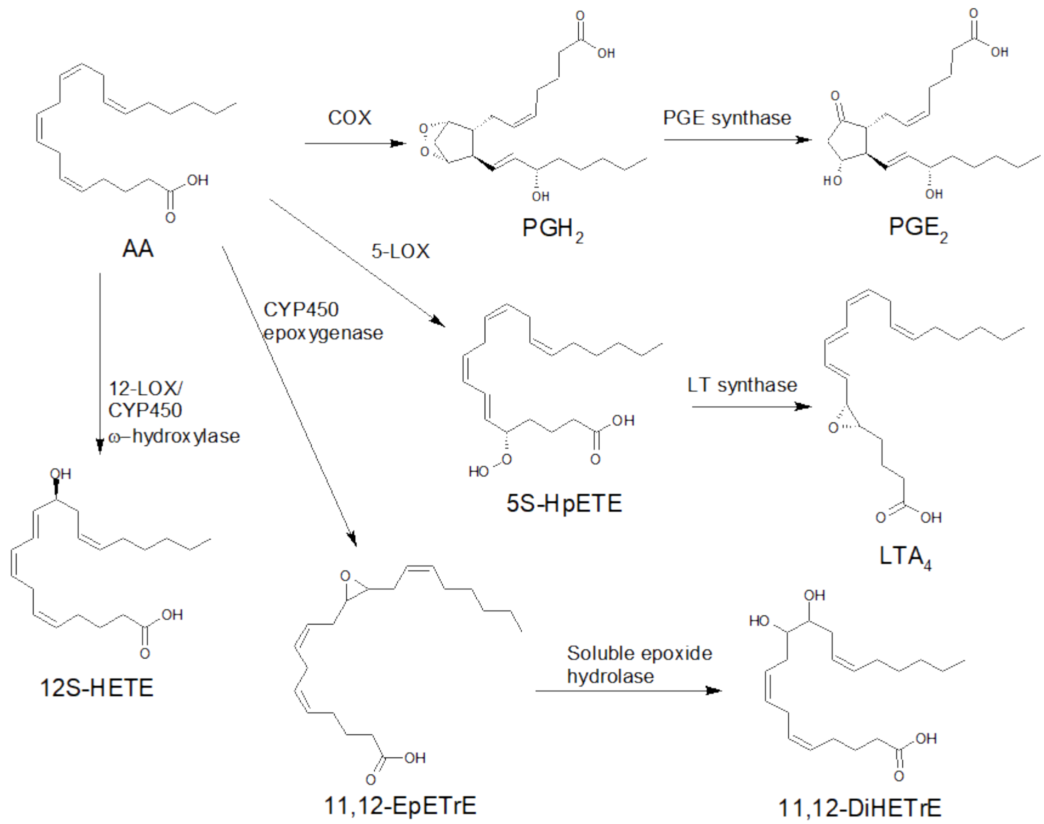

Figure 2: Some examples of arachidonic acid (AA) products of the enzymatic oxylipin synthesis pathways.

ETE) and leukotriene A4 (LTA_4) respectively. The latter is an important intermediate for the production of leukotrienes [6, 7, 8].

In the CYP450 pathway, epoxy products such as epoxyeicosatrienoic acid (EpETrE) is generated by CYP450 epoxygenase, while hydroxy products like hydroxyeicosatetraenoic acid (HETE) are generated by CYP450 ω-hydroxylase. The epoxy-products rapidly undergo hydrolysis in the body, resulting in dihydroxy-metabolites such as dihydroxyeicosatrienoic acids (DiHETrEs) and dihydroxyoctadecenoic acids (DiHOME) [6, 7, 8].

The three previously described pathways primarily oxidise free, unesterified PUFAs. The products can however be re-esterified into the phospholipids and stored, where they can be released in the future. It has also been reported that PUFAs may be oxidised enzymatically while still esterified as a part of phospholipids. The protein cytoglobin has been shown to be capable of peroxidising phospholipds, and may contribute to the synthesis of oxylipins [16, 17].

Besides the enzymatic pathways, it is possible for oxilipins to be generated via non-enzymatic oxidative reactions. Isoprostanes, which were given that name because they were isomers of prostaglandins, are formed after a free radical-mediated perioxidation of AA and are considered biomarkers of oxidative stress. Other non-enzymatic oxylipins include neuroprostanes, which are formed from DHA and are biomarkers of brain disorders such as Parkinsons's disease. These metabolites are known to act as signaling molecules, resulting in pro- or anti-inflammatory effects. [14, 15]

In addition, an intermediate product may be further metabolised by cells which are incapable of generating that product. It was first discovered when indomethacin-treated endothelial cells were shown to convert platelet-derived protaglandin H_2 (PGH_2) into prostaglandin I_2 (PGI_2). This process is termed transcellular biosynthesis and represents another layer of complexity in how these lipid mediators regulate biological activity. Lipoxins are AA metabolites whose synthesis require 5-LOX and 12/15-LOX. However, only a few cells express both enzymes, and the lipoxins are primarily produced through transcellular biosynthesis. The synthesis of lipoxin A_4 (LXA_4) by platelets requires LTA_4 generated by neutrophils [10].

1.3 Role of Oxylipins in Inflammation

Eicosanoids and other oxylipins play an important role in the regulation of inflammation. Those generated from ω-3 PUFA precursors are generally regarded as more anti-inflammatory compared to ω-6 PUFA precursors. However, whether an oxidised metabolite is pro- or anti-inflammatory cannot be simply assumed based on its precursor. For example, lipoxins, a family of eicosanoids derived from AA, an ω-6 PUFA, play a role in the resolution of inflammation. One of the proposed mechanisms for the health benefits of an ω-3 fatty acid rich diet is an increase in the production of ω-3 oxylipins and a corresponding decrease of ω-6 oxylipins. Some of the most well known families involved in inflammation are prostaglandins, leukotrienes, resolvins and lipoxins, though the role of other species such as protectins and maresins has also been investigated [6, 12, 23, 24, 25].

The process of inflammation is now understood to be a process that can be characterised by two stages, initiation and resolution, and is regulated by a complex interaction of cytokines, chemokines and lipid mediators. Inflammation is initiated by vascular dilation, increased capillary permeability, increased blood flow and recruitment of leukocytes such as neutrophils. During resolution, mononuclear white blood cells at site clear debris and apoptotic cells, returning the inflammation site back to homeostasis. The resolution is an active process, not a passive as previously assumed, where inflammation ends due to a reduction of inflammatory signals. An inability to resolve inflammation can result in persistent and chronic inflammation, which is the cause of many inflammatory diseases [23]. In autoimmune diseases, the overreaction of the immune system to cells and organs of the body causes an uncontrolled, chronic inflammation, resulting in damage to the affected tissues [25].

During the course of inflammation, alterations of the lipidomic profile have been observed. Immune cells, platelets and endothelial cells generate eicosanoids such as prostaglandins, leukotrienes, thromboxanes, which are involved in the initiation of inflammation. During the resolution of inflammation, oxylipins such as lipoxins, resolvins, protectins and maresins are expressed and contribute to the resolution. These lipid mediators can interact with various receptors, which include toll-like receptors (TLR), peroxisome proliferator-activating receptors (PPAR), G-protein coupled receptors and others [6, 23, 12].

Fibroblasts are also involved in inflammatory processes, producing both pro- and anti-inflammatory eicosanoids and other chemokines. These cells are long-lived and have been identified as an important component in chronic inflammation. The group had previously analyzed changes in inflammatory mediators after inflammatory stimulation and treatment with dexamethasone [20].

Co-localization and expression of the enzymes determine which oxylipins are produced. The various cell types involved in the inflammation process have different oxylipin profiles. In addition, different cell types converging at site of inflammation can synthesise additional oxylipins by transcellular biosynthesis, where one cell type produces an intermediate product that is taken up by a different cell type and further metabolised [10, 12].

The inflammatory effects of many eicosanoids and related molecules have been researched extensively. They form a complex signaling network which is vital for the immune system to function effectively. The family of prostaglandins includes PGE_2, to which both proinflammatory and anti-inflammatory effects are attributed. TXA_2 is produced by platelets and promotes platelet aggregation. The leukotriene LTB_4 attracts leukocytes to the site of inflammation. Other eicosanoids such as 20-HETE and 12-HETE are also known to have proinflammatory effects [6, 12, 18].

The term specialized pro-resolving mediators (SPMs) has been used to refer to some oxylipins, such as the lipoxins, resolvins, protectins and maresins, which are derived from ω-3 PUFAs EPA and DHA. These are products of the LOX and COX pathways, which may play a key role in the resolution of inflammation by down-regulating pro-inflammatory signals, preventing neutrophil infiltration and enhancing the clearance of microbes and debris by macrophages. Many SPMs such as resolvins and maresins require sequential oxidation by different pathways and enzymes. During resolution, the production of leukotrienes by LOX, a family of eicosanoids associated with pro-inflammatory effects, is also shifted over to lipoxin [6, 12, 13].

Eicosanoids and related oxylipins also regulate endothelial cell functions during inflammation, which among others include barrier cell functions, proliferation, migration and immune cell adhesion. These endothelial cells also play a role in maintaining an anti-inflammatory environment during homeostasis, such as secreting PGI_2, a prostaglandin which inhibits platelet aggregation [19].

Prostaglandins such as PGE_2, PGI_2 and PGD_2 are also known to regulate T-cell activity and differentiation through G-coupled protein receptors. These include the prostaglandin E receptors EP2 and EP4, which trigger signalling pathways such as the cAMP pathway as well as regulating expression of prostaglandin receptors in a feedback loop. These T-cells play an important role both in maintaining homeostasis as well as contributing to inflammation. The same molecule may have different biological effects on the T-cells, which is dependent on the context of their release. PGE_2 can induce the polarisation of CD4+ T cells to Th1 and Th17 cells in combination with other cytokines such as interleukine 23 (IL-23), but is also involved in the formation of regulatory T cells from CD4+ cells [21, 22].

1.4 Oxylipins in Cancer and Autoimmune Diseases

The role of eicosanoids and other lipid mediators in cancer has been researched extensively. The prostaglandin PGE_2 is commonly upregulated by tumour cells and is known to promote the migration, proliferation and invasion of cancer cells. One of the major hallmarks of cancer is the evasion and suppression of the immune system, preventing their elimination. This can be achieved by multiple methods, such as influencing immune checkpoints and recruitment of immune-suppressive cells such as regulatory T cells (T_{reg}). The production of oxylipins in both the cancer cells and the tumor microenvironment may be an important factor in establishing immune evasion as well as promoting growth [26, 27].

Inflammation is also considered to be one of the key components during cancer development. Chronic inflammation has been linked to an increased cancer risk within the affected tissues while treatment with anti-inflammatory COX-2 inhibitors and similar drugs has been shown to reduce cancer development. Tumour associated macrophages, neutrophils, myeloid cells and dendritic cells (DCs) are all known to play a role in tumour inflammation. They release cytokines, chemokines and other signal molecules, such as the vascular endothelial growth factor (VEGF), which suppress immune response to tumour cells while promoting angiogenesis and chronic inflammation. Enzymes of the COX, LOX and CYP450 pathway were found to be upregulated in many cancers. Many of their products, such as PGE_2, 12-HETE and 20-HETE, have also been associated with tumour progression [26, 27, 28].

In one study on breast cancer patients, the oxylipins levels of 13-hydroxyoctadecadienoic aicd (13-HODE), 9-HODE, 13-hydroxy-octadecatrienoic acid (13-HOTrE), 9-HOTrE and 12-hydroxyhepta-decatrienoic acid (12-HHTrE) were found to be elevated in comparison to healthy controls [29]. Platelet activation occurs in metastatic melanoma, leading to an increase of eicosanoids in the blood, including 12S-HETE and 15S-HETE [30]. A 2020 review showed that in many solid tumours, expression of some CYP450 isoforms involved in eicosanoid synthesis was increased. These isoforms included both epoxygenases and hydroxylases such as CYP2J2 and CYP4F respectively. [31].

The immune system is responsible for defending the body against pathogens, toxins and other foreign substances. It can be generally divided between an innate system and an adaptive system. The innate immune system may be defined as the mechanisms which are already encoded in the germline genes, including physical barriers, detection of molecules characteristic of pathogens, phagocytic cells, natural killer cells and others. The adaptive immune system is capable of targeting specific antigens through the antigen receptors on T- and B-lymphocytes. The formation of these receptors is a complex process which involves the rearranging of their genes during the development of these cells. T-cells can be activated by antigen-presenting cells, with their response determined by the subtype, such as the release of cytokines and other signal molecules or cytotoxic activity against infected cells. B-cells can mature with the assistance of CD4+ T-cells, undergoing a process called isotope switching and producing highly specific antibodies targeting the antigen [32].

In autoimmune diseases, T- and B-cells targeting self-antigens are activated. As a result, T-cells produce cytokines, which enhance immune response and inflammation, while B-cells create antibodies that target the self-antigens, resulting in activation of immune cells and further inflammation at their binding site. Reactive oxygen species (ROS) are produced at the inflammation site and can lead to increased oxidative stress, which can damage lipids, proteins and deoxyribonucleic acids (DNA). The increased oxidative stress may also result in an activation of pathways involved in lipid mediator production, as well as the nonenzymatic formation of other oxylipins including isoprostanes. Studies have shown an increase of PLA_2 activity, the enzyme responsible for the hydrolysis of PUFAs from phospholipids, and COX-2 in many autoimmune diseases. The LOX pathway and its products have also been implicated, such as 15-LOX and its product 15-HETE, which may play in the pathophysiology of rheumatoid arthritis [14, 48].

There are many types of autoimmune diseases, and they can be both local or systemic. Rheumatoid arthritis is an autoimmune disease of the joints, resulting in bone and cartilage damage. Type 1 diabetes is caused by the destruction of pancreatic β-cells by the immune system. Inflammatory bowel disease is caused by autoimmune activity against the intestinal mucosae. Systemic lupus erythematosus (SLE) is caused by the immune system targeting DNA. Multiple sclerosis is an autoimmune disease of the central nervous system [25, 48].

An increased dietary uptake ω-3 PUFAs, which are associated with anti-inflammatory properties, appears to reduce the degree of autoimmunity in these diseases. Administration of SPMs in combination with NSAIDs has been proposed as a possible therapy [25].

1.5 Oxylipin Analysis

Due to the instability of oxylipins, it is important to store samples at -80°C and avoid unneccessary freeze/thaw cycles [35]. The processing of samples can have an impact on the amount of oxylipins measured due to continued formation and degradation during the process. In particular, platelet activation in blood samples can lead to a massive increase of platelet derived oxylipins, such as certain COX and 12-LOX pathway products. As a result, serum, which is obtained after clotting at room temperature, can have very different oxylipin profiles compared to plasma. Other samples such as urine, sputum, cell culture and tissue samples have also been measured [39, 47].

Anticoagulants are often added to plasma or blood samples. The inhibition of the clotting process prevents changes to the sample between collection and analytical analysis. Citrate, flouride and ethylene diaminetetraacetic acid (EDTA) achieve this by binding Ca^{2+} ions, while heparin inactivates thrombin. Additionally, anticoagulants such as EDTA which bind Ca^{2+} also inhibit PLA_2 enzymes, preventing the hydrolysis of PUFAs from phospholipids. [36, 37].

Besides free oxylipins, esterified oxylipins can also be targeted for analysis. This can be achieved by performing an alkaline hydrolysis step during sample preparation, allowing the esterified oxylipins to be extracted alongside the free oxylipins. However, this process may have an impact on the oxylipin profile. It has been reported that some prostanoids are degraded under alkaline conditions [33, 61].

Additives can also be added to samples during collection in order to prevent further changes to the oxylipin profile. Enzyme inhibitors such as various COX inhibitors prevent further synthesis or metabolism, while antioxidants such as triphenylphosphine and butylated hydroxytoluene (BHT) prevent autoxidation of oxylipins and PUFAs [35].

Due to the low concentrations of oxylipins and ion suppression from the matrix, it is neccessary to extract the analytes from the sample before analytical measurements, concentrating the analytes and reducing interference from the matrix. It is common to precipitate proteins, followed by liquid-liquid extraction (LLE) or solid phase extraction (SPE). Due to better results and ease of operation, SPE is the preferred method for sample preparation [39, 35]. There are multiple types of commercial SPE columns, with different materials and properties. Ostermann et al. compared different columns and protocols, and investigated differences in internal standard recovery rates, matrix effects and ion suppression. The use of internal standards was unable to compensate for differences in the SPE methods, which may result in two methods giving different concentrations for certain molecules. Comparing the results of two different protocols can thus be difficult [34].

Historically, eicosanoids had been analysed with gas chromatography-mass spectrometry (GC-MS) or gas chromatography-tandem mass spectrometry (GC-MS/MS). However, this required derivatization due to the presence of thermally labile functional groups. Liquid chromatography-mass spectrometry (LC-MS) and liquid chromatography-tandem mass spectrometry (LC-MS/MS), which do not require additional derivatization steps, are now widely used for analysis of oxylipins. However, a 2014 review pointed out that the limit of quantification (LOQ) in many LC-MS methods are several times higher than that of GC-MS methods [38, 40].

Separation of eicosanoids and related molecules in HPLC methods is usually carried out based on their hydrophobicity using a reversed phase column. Better separation can be achieved by selecting conditions, such as the composition of the mobile phase and gradient, which are optimal for the class of oxylipins which is being investigated [40].

Chiral chromatography may be able to separate stereoisomers and closely eluting substances better than reversed phase chromatography. However, this method has some disadvantages, such as lower sensitivity and long run times. Thus it is mainly employed for targeted analysis of known compounds [40].

A difficulty in the analysis of oxylipins is the large variety of isomers with similar structures and chemical properties, making them difficult to identify correctly without access to analytical standards. There has been success with predicting the molecules by performing fragment pattern analysis of the MS/MS spectra, with one group reporting the screening of over 100 lipid mediators [40, 45]. Another group worked on computer chemical networking to evaluate LC-MS/MS data and identified over 500 known as well as 46 putative compounds [41].

Ion mobility is another property which can be used to separate closely eluting and coeluting molecules by adding another analytical dimension. Oxylipins have already been successfully characterised using ion mobility mass spectrometry methods [40, 42, 43]. In these methods, ions within an electrical field drift through a buffer gas before being analysed with a mass spectrometer. The drift time is dependent on the interactions of the ions with the gas molecules, which can be described by their mobility K. This is dependent on many factors, including buffer gas temperature, pressure and collisional cross section of the ions. The latter can be derived from K and could be useful for structural analysis. There are multiple methods to perform ion mobility spectrometry, which has contributed to difficulties when comparing results, though there have been efforts to standardise definitions, references and reporting of results. In some methods, the ion passes through a stationary gas to the detector. In others, the ion passes through a moving gas, such as as trapped ion mobility spectrometry (TIMS), where a moving gas and electric field trap the ions in position until they are eluted by changing the electric field [44].

For quantification, there are multiple methods, each with their own advantages and disadvantages. In the background subtraction method, a pooled matrix representative of the sample matrix is used to generate a calibration curve. The disadvantages of this method are reproducibility issues between batches of pooled matrixes and a LOQ which is limited by the analyte concentration within the pooled matrix. In the standard addition method, aliquots of the samples are spiked with different amounts of the analyte to generate a calibration curve, from which the concentration within the sample can be derived. However, this method requires a large quantity of each sample and can be time-consuming to carry out [46, 39].

If the composition of the biological matrix is known, it may be possible to generate an artificial matrix with similar properties and use the artificial matrix generate a calibration curve. Alternatively, stripping a biological matrix of analytes, such as using activated coal or heat decomposition, is another method of generating an analyte-free matrix, but this process may change other properties as well. The changes in composition could cause the extraction recovery and matrix effect to be different than the original [46, 39].

A stable-isotope-labeled standard can also be added to the sample as a surrogate analyte. Since it has similar chemical and physical properties, the retention times, recovery and signal intensities should be nearly identical to the analyte. However, these stable-isotope-labeled standards are costly and may degrade after prolonged storage [46, 39]. Due to the impracticality of obtaining standards for every analyte, a single stable-isotope-labeled standard might be used to quantify a group of similar oxylipins [35].

1.6 Extracorporeal Photopheresis

Extracorporeal photopheresis (ECP) is a therapy method that has been employed for cutaneous T-cell lymphoma (CTCL) since FDA approval in 1988. It has also been used to treat inflammatory skin conditions, such as psoriasis, and has been investigated as a possible therapy for various autoimmune diseases. During this procedure, the buffy coat is separated from the patient's blood and exposed to ultraviolet-A (UVA) radiation (wavelength around 320-400nm). The photosensitivising agent 8-methoxypsoralen (8-MOP) is added for the latter step. After treatment, the irradiated cells are reinfused back into the patient. A big advantage of ECP lies in its low toxicity and side effects, as well as not suppressing the immune system. Treatment of autoimmune diseases with immunosuppression, such as with steroids, usually leads to severe side effects, such as toxicity or infectious complications [49, 62, 63].

CTCL refers to a group of diseases which are characterised by proliferation of monoclonal T-lymphocytes involving the skin. The most common subtypes are mycosis fungoides and Sezary syndrome. In mycosis fungoides, the proliferation of memory T-cells in the skin results in the formation of skin lesions and plagues. Progression of the disease results in these spreading over body. Sezary syndrome refers to a leukemic variant of CTCL with Sezary cells, atypical cells with a cerebriform nucleus. This variant has a poor prognosis, with a 5-year rate survival rate of 28% or less [49, 50] .

ECP treatment usually takes place on two consecutive days on a biweekly or weekly schedule. The total length depends on the disease [49, 52]. There is no standardised method for performing ECP, instead the different commercial products each have their own protocol. The UVA intensity is around 2 J/cm^2. The ECP treatment methods can be divided into inline and offline methods. The inline method performs all the steps within a single instrument while maintaining a constant flow, while offline treatments perform the steps sequentially on different machines. The number of steps that are required as well as treatment lengths can thus vary from protocol to protocol. While the inline methods require less steps and are faster, they may also require greater extracorporeal volumes, which is important for patients with low body weight and hematocrit. It has also been shown that different ECP methods have differing rates of apoptosis and number of cells collected [51, 52].

During this treatment, 8-MOP intercalates with the DNA in the white blood cells. Photoexcitation with UVA results in 8-MOP binding to the DNA base thymine, with further reactions leading to DNA crosslinking. This DNA damage induces apoptosis in many of the cells [63, 54]. Only around 5 % of white blood cells in the body are exposed to the treatment. Treated lymphocytes undergo apoptosis within 72 h, while treated monocytes, which comprise around 30 % of the treated cells, appear to be activated. However, these monocytes also appear to have reduced differentiation to immature DCs, which also seem to be incapable of maturation [62, 63].

Under ECP conditions, plasma lipids and proteins do not appear to suffer significant oxidative damage, indicating that the antioxidative capacity of plasma is able to cope with the oxidative stress, though ROS may still be generated [55].

The mechanism behind ECP therapy is not well understood, though it may be linked to a shift in the immune system. Studies have shown that ECP causes an increase in CD36+ macrophages, changes in the cytokine profile such as a decrease of tumour necrosis factor alpha (TNF-α), shifts in the balance of the T-helper cells between Th1 and Th2, and higher T_{reg} counts [49, 53, 63]. One theory proposes that apoptotic lymphocytes cells may be phagocytosed after ECP, resulting in a stimulation of the immune system. DCs, an antigen-presenting cell, play an important role in activating T cells and priming them against the presented antigen. The interaction of platelets adherent to the equipment surfaces and monocytes may stimulate the differentiation of monocytes into DCs, and has also been suggested as a possible mechanism [49, 53, 63]. However, other sources reported that most monocytes and immature DCs also undergo apoptosis after ECP, and surviving immature DCs have a greatly reduced ability to mature [56].

The effects of differing 8-MOP protocols on the apoptosis rate of leukocytes has also been studied. Preincubation of leukocytes with 8-MOP for half an hour lead to a significantly increased apoptosis rate after ECP compared to the addition of 8-MOP immediately before UVA irradiation [57].

Another study examined the mechanical stresses of ECP. Samples which only underwent the apheresis process without addition of photosensitisers or UV treatment were compared with blood samples obtained directly from patients. No significant effect on the apoptosis or proliferation of mononuclear cells was found. This is in contrast with samples which underwent ECP, which showed a significant increase in apoptosis and an inhibition of proliferation. These results showed that the mechanical stresses by themselves were not responsible for the apoptosis observed after ECP. [59].

Besides CTCL, ECP has been investigated as a treatment for a number of autoimmune diseases, where good responses were observed in many cases, such as transplant rejection, graft vs host disease (GVHD) and systemic sclerosis. Prophylactic use of ECP for some diseases, such as transplant rejection, is also under consideration [49, 62, 63]. One difficulty in evaluating the effectiveness of ECP treatment lies in the large variety in treatment methods and schedules, which could impact an accurate assessment [51, 52, 62].

At the time this was written, very few studies on changes to the eicosanoid and oxylipin profile after ECP therapy could be found.

In one study, UV-irradiated AA and EPA were shown to increase apoptosis within HL-60 caucasian promyelocytic leukemia cells, likely through interactions with the mitochondria. The formation of conjugated diene products, a peroxidation product, during UV-irradiation was also measured [60]. In another study, a large increase of HETEs, in particular 5-HETE, was observed in plasma after ECP, likely produced via non-enzymatic oxidation processes. Before the second ECP treatment, HETE levels in patients had returned to baseline levels. However, after treatment on the second day, the increase of HETEs was reported to be longer lasting and could still be observed on the third day. In this particular study, alkaline hydrolysis was carried out on the plasma samples, releasing esterified HETEs [61].

1.7 LC-MS and Orbitrap

High-performance liquid chromatography-mass spectrometry (HPLC-MS) combines the chromatographic separation of a HPLC method with a mass spectrometer detector. Not only can the retention times of the analytes be used for identification, the chromatographic separation also greatly helps with the intepretation of mass spectra data.

Chromatography is based on the separation of components through interactions with a stationary phase and a mobile phase. Most HPLC devices load samples with a loop injector, also termed valve injector. The sample is loaded onto a sample loop while the liquid mobile phase continues flowing through the HPLC column, which acts as the stationary phase. It is possible to fill the loop partially. To bring the sample onto the column, a device rotates, bringing the flow of the mobile phase through the sample loop, flushing the contents onto the column [64, 65].

Most HPLC columns contain tightly packed silica particles, whose properties are usually obtained through chemical modification. One such modification is the bonding of a C18 group, which is used for reversed phase HPLC. Smaller particle sizes increase the efficiency of the column, but require higher pressures and are also more susceptible to contamination and clogging

[64, 65].

Ultra-high performance liquid chromatography (UHPLC) is an advancement of HPLC which uses even smaller particles, which can be less than 2 µm in size. While this increases performance and permits a higher mobile phase velocity, the small size of the particles also results in a greater pressure drop, neccessitating far greater pressures than in HPLC [66].

In isocratic elution, the composition of the mobile phase stays constant throughout the run, which can lead to long retention times if some analytes are retained strongly by the column. Gradient elution varies the composition of the mobile phase over the course of the run, gradually shifting to a composition which elutes the analytes better. Buffers are present in the mobile phase to control the pH. In HPLC-MS, volatile buffers are neccessary due to the coupling with a mass spectrometer [64, 65].

The eluting analytes can be measured by a number of different instruments, such as UV detectors, electrochemical detectors or mass spectrometers. The resulting chromatogram plots the signal intensity against the retention time. The total-ion-current (TIC) measures the sum intensity of all ions, while extracted ion chromatograms, also termed reconstructed ion chromatograms, only contain one m/z. A spectrum can also be obtained, which plots the signal intensity against the m/z at a given time point [64, 65].

Quantification of the chromatographic peaks is dependent on the limit of detection (LOD), limit of quantification (LOQ), signal noise, as well as the linear and dynamic ranges of the analyte. The linear range is the range where the signal is proportional to the concentration, while in the dynamic range the signal still increases, but no longer proportionately, to an increase in concentration. Quantification can be carried out with external standards, standard addition or internal standards. In HPLC-MS, it is advantageous to use isotopically labelled analytes as internal standards. They would experience a similar loss as the analytes between sampling and analysis, possess similar chromatographic and ionisation properties while still being differentiated by their different masses [64, 65].

After analytes are ionised by a suitable technique, mass spectrometers measure the mass-to-charge ratios (m/z) of the resulting ions and their intensity. These properties are used for the identification and quantification of the analytes. Mass spectrometers require a high vacuum to prevent ions from colliding with air molecules. However, the flow of mobile phase in HPLC would overwhelm the mass spectrometers if connected directly. Instead, interfaces are required which both ionise the analytes and remove all or most of the mobile phase. Volatile buffers are also required, as inorganic or nonvolatile buffers would clog up the interface or interfere with mass spectrometer. Ion suppression may also occur, as both analytes and non-analytes compete for ionisation [64, 65].

Electrospray ionisation (ESI) and atmospheric pressure chemical ionisation (APCI) are widely used as interfaces in HPLC-MS. In ESI, the eluting mobile phase passes through a capillary under high voltage, forming highly charged droplets which rapidly evaporate. After reaching a small enough size, the repulsive forces of the charges on the surface overcomes the surface tension. The resulting Coulombic explosions generate smaller droplets until each only contain a single ion. Evaporation of the remaining solvent then leaves the ions in a vapour phase, which are focused into the mass spectrometer. In APCI, the eluting mobile phase first passes through a nebulizer and is dried by a heater region. Afterwards, a corona discharge ionises the gaseous solvent, resulting in chemical ionisation of the analytes by reactions with the ionised solvent [64, 65].

Modern mass spectrometers are capable of tandem mass spectrometry (MS/MS), where two mass spectrometry stages are combined to obtain more information about the analyte by fragmenting the ions between the stages. There are multiple methods of MS/MS, which may also be dependent on the instrument used. Triple quadrupole mass spectrometers can be set to the product ion scan mode, where a precursor m/z is selected, fragmented and the fragment ions are analyzed. In precursor ion scan mode, it is the second stage which selects a specific m/z while the first stage scans through the mass range. In constant neutral loss scan mode, the m/z scanned by the different stages are set to a constant distance. In selected reaction monitoring (SRM), also termed multiple reaction monitoring (MRM), both stages only measure predetermined m/z [64, 65].

Targeted mass spectrometry methods aim to analyse specific analytes, while untargeted methods seek to cover as many analytes as possible, including unknown ones. Mass spectrometry spectra databases can be used to build a library of transitions for SRM. When combined with scheduled acquisition, where the analyte is only monitored around the expected retention time, this allows for a highly sensitive and selective targeted analysis of a sample. One disadvantage of such targeted methods is the poor coverage of unknown analytes. Data from untargeted mass spectrometry methods may be used to build a library of transitions for targeted methods. In the untargeted data-dependent acquisition (DDA) method, ion fragmentation is only carried out on precursor ions which fulfill conditions such as having the highest signal intensity. Data-independent acquisition (DIA) instead simultaneously fragments all precursor ions and measures the resulting product ions. Sequential windowed acquisition of all theoretical fragmentation spectra (SWATH) is a variant of DIA where mass range windows covering the entire precursor mass range are scanned. While the untargeted methods can have a greater analyte coverage than targeted methods, data processing is also more complicated [68, 67].

There are many different types of mass spectrometers with their own advantages and disadvantages. High resolution, accurate mass spectrometers (HR/MS), which include Fourier-transform ion cyclotron mass spectrometry (FT-ICR) and Orbitrap, are capable of determining the atomic composition of the analyte by measuring its exact mass [69, 70]. As an Orbitrap mass spectrometer was used in this master's thesis, it will be further described below.

The Orbitrap mass analyzer is a HR/MS instrument, which functions by trapping ions in an electric field generated by a central spindle-shaped electrode and two symmetrical outer electrodes. The latter also act as receiver plates for image current detection. The ions are first accumulated in the radiofrequency-only bent quadrupole of the C-trap device, and injected into the Orbitrap by ramping down the radiofrequency voltage and applying a high-voltage pulse. After being injected into the Orbitrap, the velocity of the ions and the radial electric field cause the ions to oscillate around central electrode, which generates the image current in the receiver plates. The mass spectrum is obtained through Fourier transformation of this time-domain signal [69, 70].

The first commercial instrument with an Orbitrap mass analyzer was introduced in 2005 with a linear ion trap for precursor isolation and fragmentation. The Q Exactive mass spectrometer, which was introduced in 2011, instead used a quadrupole for precursor isolation and fragmented precursor ions by higher-energy collision-induced dissociation (HCD). HCD is performed with a gas-filled quadrupole after the C-trap, which is capable of greater collision energy than a linear ion trap, generating more fragment ions. In addition, an advanced signal processing algorithm termed enhanced Fourier transform (eFT) enabled an increase of the resolution [69, 70].

The Q Exactive HF mass spectrometer features improvements over the original Q Exactive mass spectrometer. A low resolution pre-filter in the injection flatapole reduces unwanted ions and the new segmented quadrupole has improved isolation and transmission. The ultra-high-field Orbitrap mass analyzer is also smaller, enabling a higher field strength, increased frequency of the ion oscillation and thus an increased resolution as well as shorter scan times [71].

2 Materials

2.1 Chemicals

LC-MS grade solvents H_2O, MeOH, ACN as well as FA were obtained from VWR International GmbH. Absolute ethanol (99.9 %) was obtained from AustrAlco GmbH.

Deuterated standards were purchased from Cayman Europe and stored at -80°C. These were 15S-HETE-d8, 12S-HETE-d8, 5S-HETE-d8, 20-HETE-d6, 5-Oxo-ETE-d7, PGE_2-d4, 11,12-DiHETrE-d11, 14,15-DiHETrE-d11, and 8-iso-PGF_2-d4.

For the method development, standards were purchased from Cayman Europe. These were 20-HETE, 11S-HETE, 9-HETE, 13R-HODE, 13-hydroxydocosahexaenoic acid (13-HDoHE), 7-HDoHE, 9R-HODE, 17-HDoHE, 8-HDoHE, 18-HEPE, 8-HEPE, 9-HEPE, 5-HEPE, 13-oxooctadecadienoic acid (13-Oxo-ODE), 10-HDoHE, 20-HDoHE, 11-HDoHE, 4-HDoHE, 12-epi-LTB4, 8S-HETE, 5-Oxo-ETE, 12-HEPE, 5S-HETrE, 6-trans-LTB4, 13S-HpODE, 14,15-DiHETrE, 11,12-DiHETrE, 8,9-DiHETrE and 5,6-DiHETrE.

2.2 Instruments and Containers

Calibrated pipettes from Eppendorf and Gilson and pipette tips from Greiner Bio-One International GmbH were used for pipetting. The SPE columns Strata^{TM}-X 33 µm Polymeric Reversed Phase, 30 mg/1 mL tubes were obtained from Phenomenex Inc.. 1.5 mL screw neck glass vials, screw caps for 1.5 mL glass vials and 200µl glass inserts were obtained from Machary-Nagel GmbH. The Vacmaster^{TM} manifold for SPE was obtained from Biotage. 15 mL Falcon^{TM} Conical Centrifuge tubes were obtained from Corning^{TM}. The miVac Duo concentrator was obtained from GeneVac Ltd.. For the UHPLC-MS/MS analysis, a Vanquish UHPLC system from Thermo Scientific^{TM} equipped with a Kinetex C18 (2.1 mm x 150 mm, 2.6 µm) reversed phase UHPLC column from Phenomenex Inc. was used and coupled with a Q Exactive^{TM} HF Hybrid Quadrupole-Orbitrap^{TM} Mass Spectrometer from Thermo Scientific^{TM}. A Kinetex C18 (2.1 x 100mm, 1.7 µm) reversed phase UHPLC column from Phenomenex Inc. was also used for the method development section.

2.3 Prepared Solutions

For the UHPLC-MS/MS method used in the analysis of ECP plasma samples, two mobile phases were prepared. Mobile phase A contained 0.2 % formic acid (FA) in H_2O. Mobile phase B contained 10 % MeOH and 90 % ACN with 0.2 % FA.

Two different deuterated standardmixes were prepared and stored at -80°C. *StandardmixPre* contained 200 ng/mL 15S-HETE-d8, 200 ng/mL 12S-HETE-d8, 200 ng/mL 20-HETE-d6, 600 ng/mL 5-Oxo-ETE-d7, 400 ng/mL PGE_2-d4, 200 ng/mL 11,12-DiHETrE-d11 in ACN. *StandardmixPost* contained 200 ng/mL 5S-HETE-d8, 200 ng/mL 14,15-DiHETrE-d11, 400 ng/mL 8-iso-$PGF_2\alpha$-d4 in ACN. *StandardmixPre* is added to the sample before protein precipitation and sample preparation. *StandardmixPost* is part of the reconstitution solution, and serve to monitor the performance of the UHPLC-MS/MS as well as degradation while in storage.

The reconstitution solution, in which the analytes are dissolved after SPE and injected onto the UHPLC column, contained 5 µL *StandardmixPost* and 145 µL (65% mobile phase A and 35% mobile phase B) with a final volume of 150 µL. This solution was freshly prepared in a sufficiently sized batch for all samples.

As part of the UHPLC method development, different mobile phases and reconstitution solutions were prepared. Mobile phase A consisted of 70 % H_2O, 30 % ACN with 0.02 % acetic acid. Mobile phase B consisted of 50 % isopropanol, 50 % ACN and 0.02 % acetic acid. The reconstitution solution consisted of 135µl (20% MeOH and 80% H_2O) and 5 µL each of StandardmixPre and StandardmixPost (both in ACN) with a final volume of 145 µL.

3 Methods

3.1 Sample Collection

Samples were collected with written consent from 6 patients undergoing ECP treatment by Ass.-Prof. Dr. Verena Paulitschke and Dr. Ara Cho from the Department of Dermatology at the Medical University of Vienna, who obtained approval from an ethics committee. Their medical history included heart transplants, CTCL, systemic sclerosis and GVHD. Blood samples were taken during the two consecutive days of treatment at the Vienna General Hospital shortly before and after the ECP treatment, collected in blood collection tubes containing EDTA and centrifuged to obtain plasma samples. The total of 24 samples were stored at -80°C.

3.2 Sample Preparation

500 µL plasma in 15 mL centrifuge tubes was spiked with 5 µL *StandardmixPre* followed by the addition of 2 mL absolute ethanol in order to precipitate plasma proteins. The samples were stored at -20°C overnight or longer to complete the precipitation. Prior to SPE, the samples were centrifuged for 30 min at 4°C and 5000 rpm. The supernatant was transferred to new 15 mL centrifuge tubes, leaving behind the protein pellet. As ethanol would prevent the binding of the analytes to the SPE column, the samples were placed in a miVac Duo concentrator at 37°C until the volume was reduced to the original volume of 500 µL. This process took around one and a half hours.

3.3 Solid-Phase Extraction

Solid-phase extraction (SPE) was performed with Strata^{TM}-X 33 µm Polymeric Reversed Phase, 30 mg/1 mL SPE columns and a VacMaster^{TM} manifold. The columns were washed with 2x1 mL MeOH followed by conditioning with 2x1 mL H_2O. Care was taken to ensure that the column did not run dry until the final elution step. A pasteur pipette was used to load the sample onto the column, which was positioned on the SPE manifold. A weak vacuum was used to gently pull the mobile phase through the column, binding the analytes. The centrifuge tube which contained the sample was washed twice with 2 mL H_2O, which were also loaded onto the column. Finally, 1 mL H_2O was added directly onto the column. To elute the analytes bound to the stationary phase, the column was briefly allowed to run dry before adding 500 µL of elution solution (2% FA in MeOH). The sample was eluted into a 1.5 mL glass vial under gentle pressure with a syringe and stored on ice until the next step. The solvent was removed by placing the samples under a constant nitrogen flow at room temperature, a process that took around 1 h. The dried samples were then stored on ice and reconstituted by adding 150 µL of reconstitution solution (see section *Prepared Solutions*) to the 1.5 mL glass vial, followed by vortex mixing and transferring the solution to a 200 µL glass insert. Immediately afterwards, the samples were stored at 4°C in the UHPLC-MS autosampler for measurement.

3.4 UHPLC-MS/MS analysis

The UHPLC-MS/MS method used to analyse the ECP samples had already been used for eicosanoid analysis previously by the group [9]. UHPLC-MS/MS analysis of the samples was carried out with a Vanquish UHPLC system from Thermo Fisher Scientific coupled to a Q Exactive™ HF Hybrid Quadrupole-Orbitrap™ Mass Spectrometer. A Kinetex C18 (2.1 mm x 150 mm, 2.6 µm) column from Phenomenex was used for UHPLC. The method was set to a flow speed of 200 µL/min, an injection volume of 20 µL and a column temperature of 40°C. Gradient elution was performed with two mobile phases. Mobile phase A contained 0.2 % formic acid (FA) in H_2O. Mobile phase B contained 10 % MeOH and 90 % ACN with 0.2 % FA. The following gradient was used: From 0 to 1 min at 35 % B, from 1 to 10 min at 35 % B to 90 % B, from 10 to 10.5 min at 90 % B to 99 % B, from 10.5 to 15.5 min at 99 % B, from 15.5 to 16 min at 99 % to 35 % B and for re-equilibration of the column from 16 to 20 min at 35 % B.

For mass spectrometry, ionisation was was carried out with heated electrospray ionisation (HESI) in negative ion mode with the following settings: capillary temperature of 253°C, spray voltage of 2.2 kV, sheath gas set to 46 units, aux gas set to 10 units. For MS2, collision energy was set to 24 eV and the method was set to a Top 2 DDA method. The MS1 resolution was 60000 at 200 m/z and the MS2 resolution was 15000 at 200 m/z.

Two technical replicates for each sample were measured. Between each photopheresis sample, a run was carried out with 20 µL H_2O to detect possible carryover. Every ten samples an aliquot of the reconstitution solution without sample matrix was measured in order to monitor variations in the instrument or degradation of the standards.

3.5 Data Processing

Peak identification based on retention times and MS2 spectra was performed with Xcalibur Qual Browser version 4.1.31.9 from Thermo Fisher Scientific. Previous experiments and standards were consulted to identify the analytes, as well as mass spectrometry databases such as Lipid Maps Structure Database and Human Metabolome Database [73, 74]. Identification was based on retention time and MS2 spectra. The retention times of the deuterated standards, which were known from previous experiments, were used as references.

Identified molecules with peaks of sufficient quality (minimum peak width of 3 s, minimum peak height of 10^4, within 5 ppm of m/z) were quantified with the Skyline program version 20.2.0286 from MacCoss Lab Software [75]. The peak area was calculated as the normalised area under curve (nAUC) of the average of the nine deuterated standards. For each sample, the average of the two technical replicates was used for further statistical analysis.

Statistical analysis was carried out using the OriginPro 2021 software version 9.8.0.200. The fold change of the analytes before and after ECP on each day was calculated as the difference divided by the average value in the samples before ECP treatment. To test the significance of the fold change, a paired t-test was carried out, comparing the samples before ECP therapy with the samples from the same patients after ECP therapy on each day. A p-value of less than 0.05 was considered significant. The Kolmogorow-Smirnow test was done out beforehand to confirm that the distribution of values did not reject normality, which is a requirement for the paired t-test.

The OriginPro software was also used to generate graphs of the results [76].

3.6 Method Development

As part of the master's thesis, a UHPLC-MS/MS method was developed based on a UHPLC-MS/MS method described by Lagerborg et al. for the analysis of bioactive lipids. This developed method was compared with the UHPLC-MS/MS method used for the analysis of ECP samples described above [72]. Standard solutions of varying concentrations were prepared and measured with both methods. The developed method would have a shorter runtime, allowing for a larger throughput of samples.

Five series of solutions containing a mixture of standards, with the concentrations 500 ng/mL, 100 ng/mL, 50 ng/mL, 30 ng/mL, 10 ng/mL, 5 ng/mL and 1 ng/mL in ACN, were prepared.

These standards were 20-HETE, 11S-HETE, 9-HETE, 13R-HODE, 13-HDoHE, 7-HDoHE, 9R-HODE, 17-HDoHE, 8-HDoHE, 18-HEPE, 8-HEPE, 9-HEPE, 5-HEPE, 13-Oxo-ODE, 10-HDoHE, 20-HDoHE, 11-HDoHE, 4-HDoHE, 12-epi-LTB4, 8S-HETE, 5-Oxo-ETE, 12-HEPE, 5S-HETrE, 6-trans-LTB4, 13S-HpODE, 14,15-DiHETrE, 11,12-DiHETrE, 8,9-DiHETrE and 5,6-DiHETrE. The compositions of the standard-mixtures are listed in Table 2.

For measuring a standard-mixture with the developed UHPLC-MS/MS method, 5 µL of the standard-mixture (in ACN) was added to a reconstitution solution consisting of 135µl mixture (20% MeOH and 80% H_2O) and 5 µL each of StandardmixPre and StandardmixPost (both in ACN). The final solvent concentration was 10 % ACN, 18 % MeOH and 72 % H_2O.

The new method used the same Vanquish UHPLC system from Thermo Fisher Scientific coupled to Q Exactive™ HF Hybrid Quadrupole-Orbitrap™ Mass Spectrometer as the original method. However, a different column, the shorter Kinetex C18 (2.1 x 100mm, 1.7 µm) column from Phenomenex with a smaller particle size was used. The mobile phase A consisted of 70 % H_2O, 30 % ACN with 0.02 % acetic acid, while mobile phase B consisted of 50 % isopropanol, 50 % ACN and 0.02 % acetic acid. The UHPLC method was set to a flow speed of 400 µL/min, a 20 µL injection volume and column temperature of 20°C. The gradient was set to the following: From 0 to 0.25 min at 1 % B, 0.25 to 5 min at 1 % to 55 % B, from 5 to 5.5 min at 55 % to 99 % B, from 5.5 to 7.5 min at 99 % B and for re-equilibration of the column from 7.5 to 9.5 min at 1 % B.

While the method described by Lagerborg et al. had a flow speed of 375 µL/min and a re-equilibration time of 1 min, the developed method had a flow speed of 400 µL/min and a re-equilibration time of 2 min. The longer re-equilibration time was chosen after preliminary runs revealed that the column pressure had not yet reached the original level after just 1 min of re-equilibration.

For mass spectrometry, ionisation was was carried out with with heated electrospray ionisation (HESI) in negative ion mode with the following settings: capillary temperature of 265°C, spray voltage of 2.2 kV, sheath

Table 2: Five series of solutions containing a mixture of standards were used for method development. The standards used in each standard-mixture are listed in this table.

Standardmix	Standards in solution
Standardmix 1	20-HETE, 11S-HETE, 9S-HETE, 13R-HODE, 13-HDoHE, 7-HDoHE
Standardmix 2	14,15-DiHETrE, 11,12-DiHETrE, 8,9-DiHETrE, 5,6-DiHETrE, 9R-HODE, 17-HDoHE, 8-HDoHE
Standardmix 3	18-HEPE, 8-HEPE, 9-HEPE, 5-HEPE, 13-Oxo-ODE, 10-HDoHE
Standardmix 4	20-HDoHE, 11-HDoHE, 4-HDoHE, 12-epi-LTB4, 8S-HETE
Standardmix 5	13S-HpODE, 5-Oxo-ETE, 12-HEPE, 5(S)-HETrE, 6-trans-LTB4

gas set to 40 units, aux gas set to 15 units. For MS2, collision energy was set to 24 eV. The MS1 resolution was 60000 at 200 m/z and the MS2 resolution was 15000 at 200 m/z.

After the first measurements resulted in an unsatisfactory result (described under *Results*), the MS/MS method was switched from a Top 2 DDA to a Top 1 DDA method, increasing the scan rate, and the standard solutions were measured again. The standards were measured from the lowest concentration (1 ng/mL) to the highest concentration (500 ng/mL).

The standard mixtures were also measured with the original method used for the ECP samples described above. For each standard mixture, 5 µL of the standard mixture was added to 145 µL of the original reconstitution solution and measured.

Calibration curves for each standard were generated by performing linear fitting with OriginPro software. During the linear fitting, the intercept was set to 0 as not doing so often resulted in the program calculating a nonsensible result i.e. inserting the lowest concentration where a peak could be quantified into the calculated linear fit resulted in a negative nAUC.

The results of the original and the developed method were then compared with each other.

4 Results

4.1 Alterations of PUFA and Oxylipin Profile after ECP

Plasma samples from six patients were collected on the two consecutive days of ECP therapy shortly before and after treatment. PUFAs and oxylipins from these samples were extracted via SPE and analysed using an UHPLC-MS/MS method in order to observe any changes to the oxylipin profile.

A total of 32 peaks, which had a minimum peak width of 3 s and peak height of 10^4 in all samples, were chosen for statistical analysis. The 9 deuterated standards were also identified, with their retention times used as reference for the analytes. Identification of the analytes was performed by comparing their retention times, m/z and MS2 spectra with previous measurements and online databases.

These analytes included precursor PUFAs, oxylipins as well as unidentified isomers or isobars of both. A list of their retention times, m/z and MS2 product ions used for identification are listed in Table 3. The unidentified isomers were labeled by their m/z or a molecule with the same exact isotopic m/z and their retention time (eg. 317_9.52, AA_12.91). In cases where two molecules coeluted in the same peak and were unable to be quantified separately, they were quantified together and labeled as such (e.g. 12S-HETE/8S-HETE and 12-HEPE/8-HEPE).

AA, EPA, DHA and DPA, PUFAs which are precursors to oxylipins, were identified. The isomeric ALA and γ-linolenic acid could not be differentiated from each other due to the lack of a standard for either. As a result, their two peaks are labeled 277_12.38 and 277_12.47. Similarly, two peaks, 305_13.17 and 305_13.35, were observed with the expected m/z of dihomo-γ-linolenic acid (DGLA), but lack of a standard prevented the identification of DGLA. 275_11.74 and 275_12.14 are two peaks with the expected m/z of stearidonic acid, though further identification was not possible due to the lack of a stearidonic acid standard.

The peaks labeled AA_12.91, EPA_12.36, DHA_12.71 and DPA_13.09 are isomers of AA, EPA, DHA and DPA respectively and elute shortly after these. It is known from previous experiments that AA_12.91 is a trans-isomer of AA. It is possible that EPA_12.36, DHA_12.71 and DPA_13.09 are also trans-isomers of the PUFAs.

Various oxylipins from different classes were measured. These included eicosanoids (HETEs, HEPEs and DiHETrEs) as well as octadecanoids (DiHOMEs and HOTrEs) and docosanoids (HDoHEs).

The peak areas of these analytes were normalised to the average area of the deuterated standards in order to compare differences between samples. Table 4 lists the calculated average nAUC values and standard deviation of the analytes in the patients according to the sample collection time. The average fold change between the samples before and after ECP treatment was calculated as the difference between the two divided by the values before ECP treatment. The significance was determined with the paired-T test, with $p<0.05$ considered significant. The results are shown in Table 5. Graphs depicting the nAUCs values of the individual analytes at different time points are shown in Figure 3 to Figure 13.

A large individual variance of the PUFA and oxylipin profile between the patients could be observed. This is likely due to the different diet, personal metabolism, health conditions and medication of the patients. Due to their medical history, which include heart transplants, CTCL, systemic sclerosis and GVHD, the patients had been taking multiple different medications each. These include various immunosuppressive drugs. Four of the six patients took aspirin, which is known to be a NSAID. The small sample size meant that statistical analysis of these factors on the patients' PUFA and oxylipin profile was not feasible.

An increase could be observed in the majority of the analytes after ECP therapy on both days. However, the change was not significant for most of these analytes, even for those with an average fold change of 1 or greater. (Table 5) This may be due to the small sample size of only six patients, limiting the statistical analysis. The significantly increased analytes after ECP therapy differed greatly depending on the day. 277_12.38 and 12-HEPE/8-HEPE were the only two analytes with a significant increase after ECP therapy on both day 1 and day 2. 12S-HETE/8S-HETE, 11-HEPE and 14-HDoHE/10-HDoHE were significantly increased only on day 1. AA_12.91, DHA, 277_12.47, 275_12.14, 15S-HETE, 11S-HETE, 5S-HETE and 14,15-DiHETrE were significantly increased only on day 2.

On the first day, higher levels could be observed for most of the analytes in the samples after ECP therapy compared to the samples before. On the second day, the samples taken before the therapy showed that they had all returned to a level similar to the first day, before the therapy. Similar to the first day, an increase in peak levels could be observed for most of the analytes on the second day after ECP therapy. This indicates that changes to the PUFA and oxylipin profile in plasma after ECP therapy is only short-term, lasting for less than a day.

The PUFAs generally had a larger average fold change than the oxylipins. 277_12.47 had the largest fold change, 7.37 and 5.34 on the first and second day respectively, though only the second day was significant. Of the PUFAs and their isomers, AA, AA_12.91, LA and 275_12.14 had the least fold change, lower than 1 on both days.

Of the oxlipins, the coeluting 12-HEPE/8-HEPE had the largest fold change, 1.03 and 1.73 on the first and second day respectively, both significant. 14-HDoHE/10-HDoHE had the second largest, 0.94 and 0.93 on the first and second day respectively, though only the first day was significant. Most of the fold changes among oxylipins was less than 0.5. With the exception of 20-HETE, the remaining HETEs that were measured were significantly increased on one of the days. While the fold changes of 3-HOTrE and 9-HOTrE were not significant on both days, the fold change on the second day appeared to be a lot larger than the first day. On the first day, 3-HOTrE and 9-HOTrE had an average fold change of 0.39 and 0.26 respectively, while they were 1.52 and 1.27 on the second day. The two DiHETrEs measured, 14,15-DiHETrE and 11,12-DiHETrE, had some of the lowest fold changes, though the fold change of 0.18 of 14,15-DiHETrE on the second day was significant.

In a study from 2000, Wiswedel et al. reported an increase of HETEs in plasma after ECP treatment. [61] Here, an increase of HETEs could also be observed, though only 12S-HETE/8S-HETE was significantly increased on day 1 and 15S-HETE, 11S-HETE and 5S-HETE were significantly increased on day 2. Similarly, their observation that the HETE levels on the second day before ECP returned to the levels of the first day before ECP was also observed here. In addition, they reported that samples taken on the third day still showed an increase in HETEs compared to the baseline. Here, samples were only obtained on the two days of treatment, and it was not possible to make this observation. It should be noted that Wiswedel et al. performed an alkaline hydrolysis to also obtain esterified HETEs, while here only free HETEs were extracted and measured.

Table 3: The PUFA precursor, retention time (RT), m/z and observed MS2 product ion of quantified molecules in the ECP samples are shown here.

Molecule	Precursor	RT	m/z	MS2 product ion
AA	-	12.8	303	259
AA_12.91	-	12.91	303	259
EPA	-	12.26	301	257
EPA_12.36	-	12.36	301	257
DHA	-	12.65	327	283
DHA_12.71	-	12.7	327	283
DPA	-	12.91	239	285
DPA_13.09	-	13.09	329	285
277_12.38	-	12.38	277	-
277_12.47	-	12.47	277	-
LA	-	12.95	279	-
305_13.17	-	13.17	305	-
305_13.35	-	13.35	305	-
275_11.74	-	11.74	275	-
275_12.14	-	12.14	275	177
15S-HETE	AA	10.32	319	301
11S-HETE	AA	10.49	319	167
12S-HETE/8S-HETE	AA	10.63	319	179
5S-HETE	AA	10.83	319	115
20-HETE	AA	9.71	319	289
12-HEPE/8-HEPE	EPA	9.85	317	179
11-HEPE	EPA	9.7	317	271
18-HEPE/317_9.52	EPA	9.48	317	243
14-HDoHE/10-HDoHE	DHA	10.49	343	297
17-HDoHE	DHA	10.36	343	263
343_10.17	-	10.17	343	241
12,13-DiHOME	LA	8.48	313	183
9,10-DiHOME	LA	8.65	313	201
3-HOTrE	ALA	9.35	293	235
9-HOTrE	ALA	9.46	293	195
14,15-DiHETrE	AA	8.89	337	207
11,12-DiHETrE	AA	9.18	337	167
15S-HETE-d8	-	10.25	327	223
12S-HETE-d8	-	10.57	327	184
5S-HETE d8	-	10.77	327	116
5-Oxo-ETE-d7	-	11.31	324	280
PGE2-d4	-	5.65	355	275
20-HETE-d6	-	9.69	325	281
14,15-DiHETrE-d11	-	8.84	348	207
11,12-DiETrE-d11	-	9.13	348	167
8-iso PGf2alpha-d4	-	4.8	357	313

Table 4: The normalised area (nAUC) of molecules in the ECP samples are shown here as the average with the standard deviation.

	nAUC			
Molecule	D1 pre	D1 post	D2 pre	D2 post
AA	17.76±7.64	31.34±22.46	15.54±11.11	24.87±16.12
AA_12.91	0.74±0.23	1.08±0.63	0.67±0.36	0.87±0.39
EPA	2.22±1.91	6.86±8.83	2.04±2.02	4.48±4.54
EPA_12.36	0.1±0.07	0.37±0.41	0.1±0.08	0.29±0.22
DHA	11.64±8.51	23.76±20.98	11.64±10.53	18.84±15.15
DHA_12.71	1.13±1.7	2.93±3.29	1.2±1.82	2.36±2.62
DPA	3.72±2.26	10.01±8.82	3.78±3.23	8.64±6.38
DPA_13.09	0.81±0.31	3.34±3.02	0.73±0.54	2.35±1.98
277_12.38	1.06±0.94	3.19±2	1.06±0.94	3.56±2.05
277_12.47	0.34±0.35	2.88±3.01	0.42±0.48	2.64±2.33
LA	27.64±13.34	37.93±16.82	25.63±12.19	39.24±10.57
305_13.17	0.27±0.21	1.3±1.54	0.32±0.42	1.03±1.09
305_13.35	0.13±0.07	0.49±0.7	0.13±0.13	0.32±0.38
275_11.74	0.11±0.08	0.42±0.38	0.14±0.1	0.4±0.28
275_12.14	0.11±0.07	0.15±0.09	0.09±0.06	0.14±0.08
15S-HETE	0.23±0.09	0.28±0.12	0.21±0.09	0.3±0.1
11S-HETE	0.05±0.01	0.07±0.03	0.04±0.02	0.08±0.04
12S-HETE/8S-HETE	1.41±0.58	2.03±0.84	1.4±0.93	2.32±1.37
5S-HETE	0.18±0.05	0.19±0.07	0.16±0.06	0.19±0.08
20-HETE	0.17±0.09	0.21±0.06	0.14±0.07	0.19±0.06
12-HEPE and 8-HEPE	0.07±0.03	0.15±0.09	0.05±0.02	0.14±0.09
11-HEPE	0.07±0.03	0.1±0.04	0.06±0.02	0.11±0.07
18-HEPE/317_9.52	0.15±0.02	0.17±0.04	0.14±0.06	0.19±0.12
14-HDoHE/10-HDoHE	0.27±0.1	0.52±0.3	0.25±0.14	0.47±0.31
17-HDoHE	0.07±0.01	0.1±0.05	0.06±0.02	0.11±0.07
343_10.17	0.07±0.03	0.1±0.05	0.07±0.03	0.11±0.08
12,13-DiHOME	5.43±3.65	9.21±5.13	6.92±3.38	10.36±6.71
9,10-DiHOME	3.42±0.98	4.83±1.91	4.95±1.76	7.01±2.84
3-HOTrE	1.42±0.31	1.97±1	0.97±0.27	2.45±2.5
9-HOTrE	0.59±0.24	0.74±0.39	0.35±0.11	0.8±0.73
14,15-DiHETrE	0.31±0.05	0.36±0.11	0.32±0.09	0.38±0.12
11,12-DiHETrE	0.23±0.04	0.27±0.1	0.24±0.07	0.31±0.13

Table 5: The fold change of the molecules before and after ECP therapy are shown here. The fold change is the difference between the values before and after ECP divided by the value before ECP. The statistical significance was calculated with a paired T-test. p-values smaller than 0.05 are marked by bold text.

	Day 1 pre- and-post treatment		Day 2 pre- and post-treatment	
Molecule	Fold Change	p-value	Fold Change	p-value
AA	0.77	0.119	0.60	0.063
AA_12.91	0.45	0.172	0.31	**0.048**
EPA	2.09	0.177	1.20	0.098
EPA_12.36	2.65	0.165	1.85	0.069
DHA	1.04	0.134	0.62	**0.039**
DHA_12.71	1.59	0.134	0.96	0.116
DPA	1.69	0.141	1.29	0.075
DPA_13.09	3.14	0.088	2.20	0.065
277_12.38	2.00	**0.038**	2.37	**0.042**
277_12.47	7.37	0.082	5.34	**0.039**
LA	0.37	0.233	0.53	0.080
305_13.17	3.76	0.144	2.18	0.077
305_13.35	2.68	0.228	1.56	0.122
275_11.74	2.74	0.093	1.99	0.066
275_12.14	0.33	0.366	0.60	**0.028**
15S-HETE	0.20	0.082	0.43	**0.023**
11S-HETE	0.50	0.057	0.70	**0.028**
12S-HETE/8S-HETE	0.45	**0.019**	0.66	0.054
5S-HETE	0.06	0.215	0.15	**0.023**
20-HETE	0.22	0.449	0.36	0.124
12-HEPE/8-HEPE	1.03	**0.047**	1.73	**0.049**
11-HEPE	0.37	**0.047**	0.84	0.066
18-HEPE/317_9.52	0.13	0.161	0.32	0.146
14-HDoHE/10-HDoHE	0.94	**0.042**	0.93	0.073
17-HDoHE	0.41	0.183	0.81	0.052
343_10.17	0.34	0.074	0.71	0.147
12,13-DiHOME	0.70	0.066	0.50	0.155
9,10-DiHOME	0.41	0.093	0.42	0.226
3-HOTrE	0.39	0.315	1.52	0.189
9-HOTrE	0.26	0.547	1.27	0.200
14,15-DiHETrE	0.15	0.154	0.18	**0.041**
11,12-DiHETrE	0.20	0.221	0.29	0.080

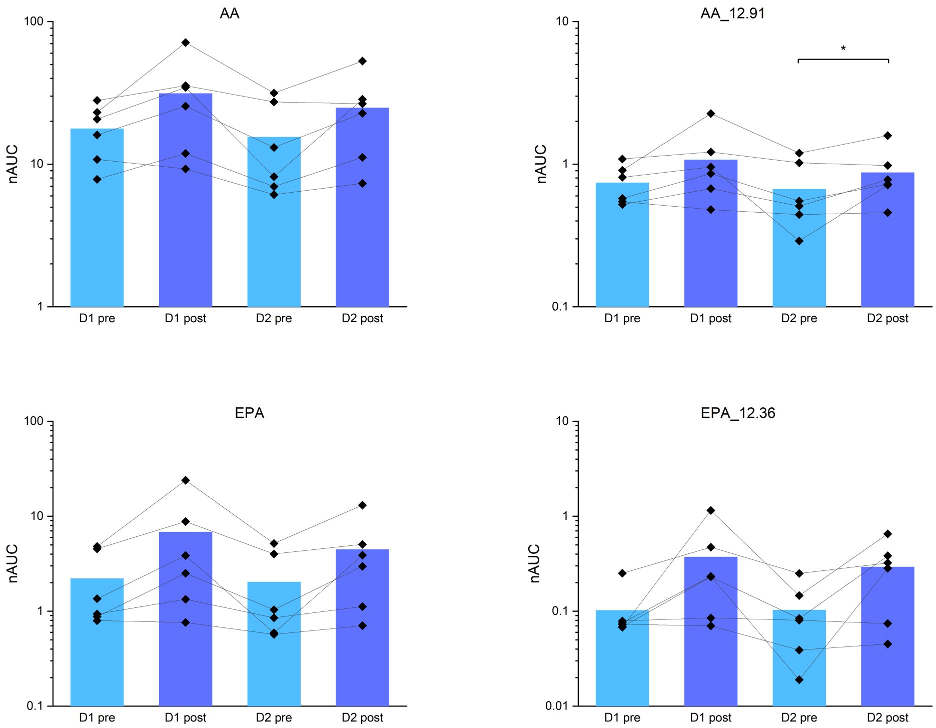

Figure 3: The normalised peak areas of AA, EPA as well as two isomers, AA_12.91 and EPA_12.36, are shown here. AA_12.91 is known to be a trans-isomer of AA. The samples were taken on two consecutive days before and after photopheresis therapy, with D1 referring to samples taken on the first day and D2 the second day. Data points belonging to the same patient are connected by a line. A significance of $p<0.05$ during the paired T-test is marked by an asterisk *.

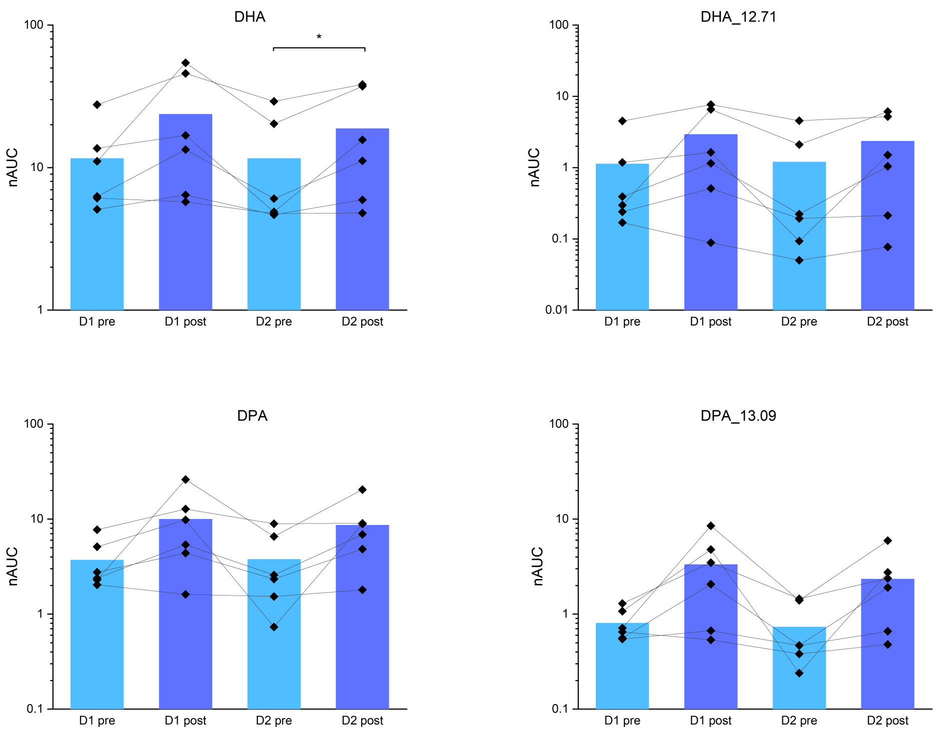

Figure 4: The normalised peak areas of DHA, DPA as well as two isomers, DHA_12.71 and DPA_13.09, are shown here. The samples were taken on two consecutive days before and after photopheresis therapy, with D1 referring to samples taken on the first day and D2 the second day. Data points belonging to the same patient are connected by a line. A significance of $p<0.05$ during the paired T-test is marked by an asterisk *.

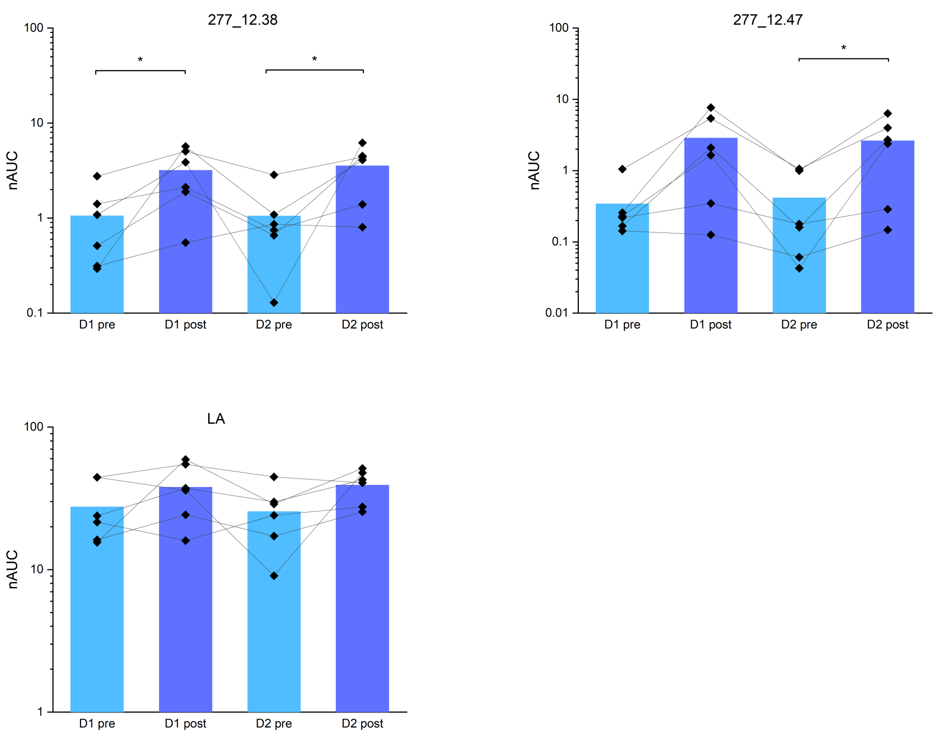

Figure 5: The normalised peak areas of LA as well as 277_12.38 and 277_12.47 are shown here. The latter two are likely ALA and γ-linolenic acid, but it is not known which molecule corresponds to the observed peaks. The samples were taken on two consecutive days before and after photopheresis therapy, with D1 referring to samples taken on the first day and D2 the second day. Data points belonging to the same patient are connected by a line. A significance of $p<0.05$ during the paired T-test is marked by an asterisk *.

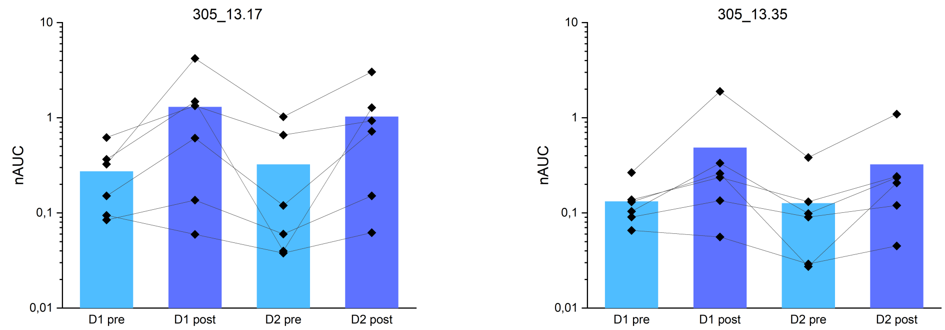

Figure 6: The normalised peak areas of 305_13.17 and 305_13.35, which have the m/z of dihomo-γ-linolenic acid (DGLA), are shown here. The samples were taken on two consecutive days before and after photopheresis therapy, with D1 referring to samples taken on the first day and D2 the second day. Data points belonging to the same patient are connected by a line. A significance of $p<0.05$ during the paired T-test is marked by an asterisk *.

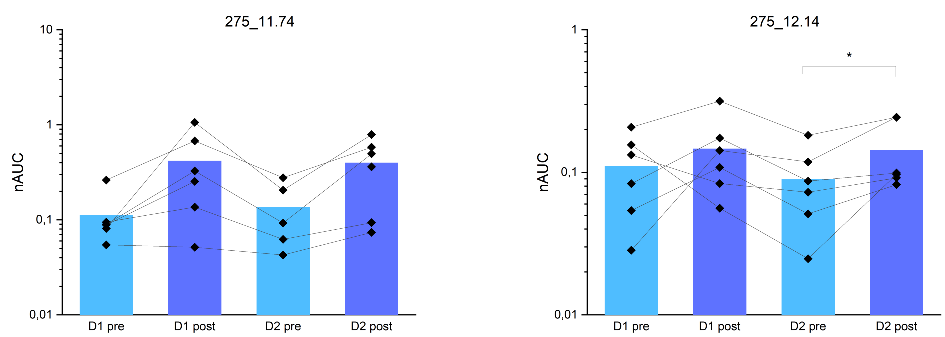

Figure 7: The normalised peak areas of 275_11.74 and 275_12.14, which have the m/z of stearidonic acid, are shown here. The samples were taken on two consecutive days before and after photopheresis therapy, with D1 referring to samples taken on the first day and D2 the second day. Data points belonging to the same patient are connected by a line. A significance of $p<0.05$ during the paired T-test is marked by an asterisk *.

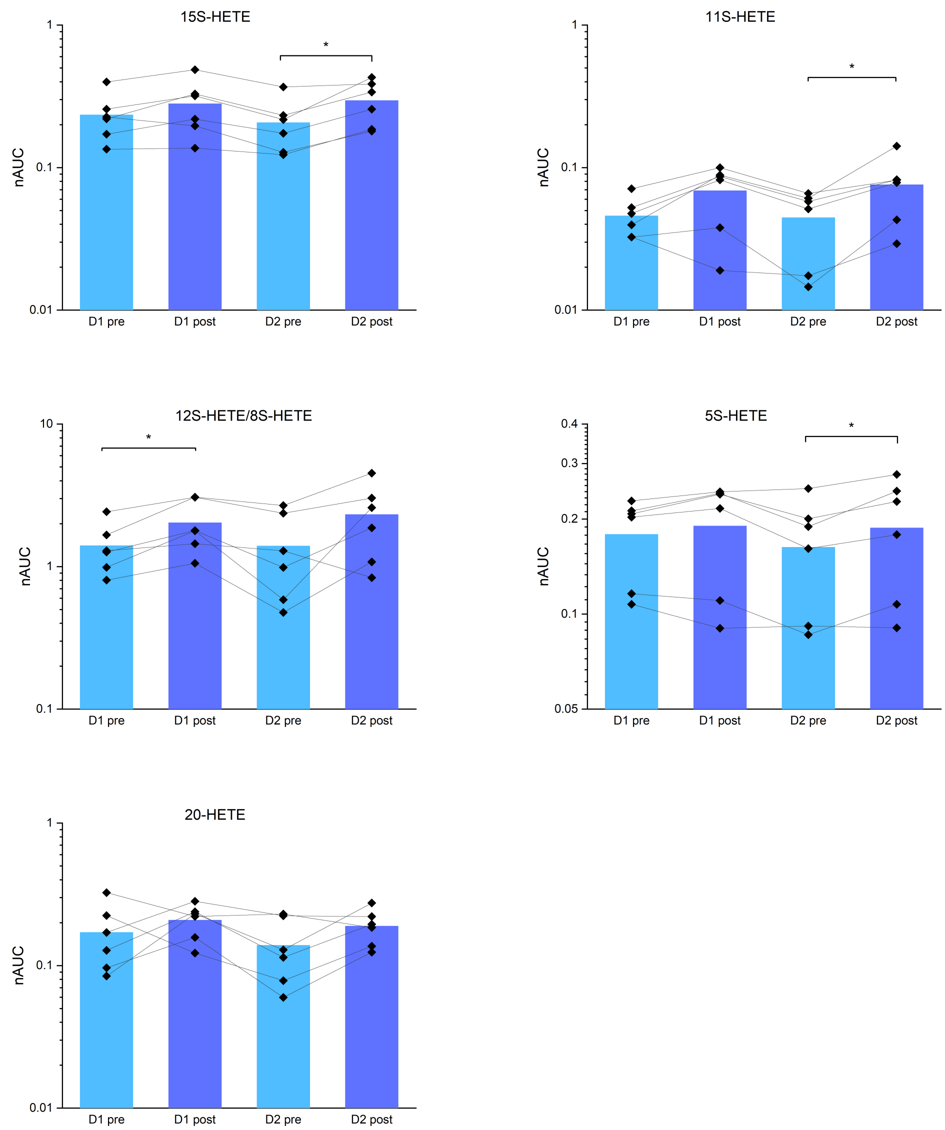

Figure 8: The normalised peak areas of identified HETEs are shown here. 12S-HETE and 8S-HETE could not be separated and were quantified together. The samples were taken on two consecutive days before and after photopheresis therapy, with D1 referring to samples taken on the first day and D2 the second day. Data points belonging to the same patient are connected by a line. A significance of $p<0.05$ during the paired T-test is marked by an asterisk *.

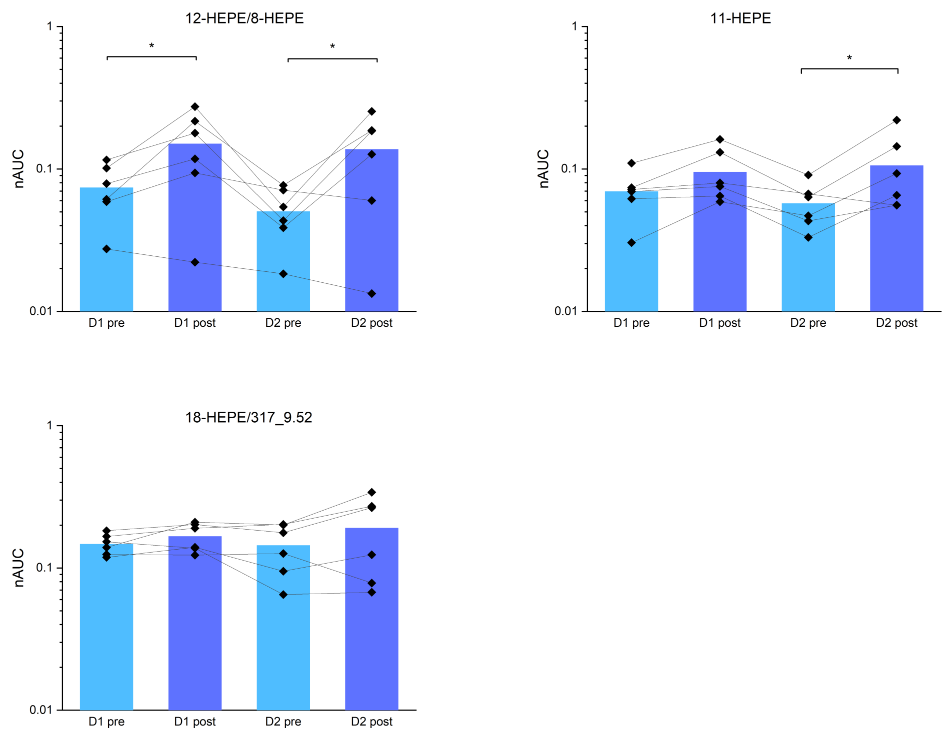

Figure 9: The normalised peak areas of identified HEPEs are shown here. 12-HEPE and 8-HEPE could not be separated and were quantified together. 8-HEPE and a HEPE isomer 317_9.52 also could not be separated and were quantified together. The samples were taken on two consecutive days before and after photopheresis therapy, with D1 referring to samples taken on the first day and D2 the second day. Data points belonging to the same patient are connected by a line. A significance of $p<0.05$ during the paired T-test is marked by an asterisk *.

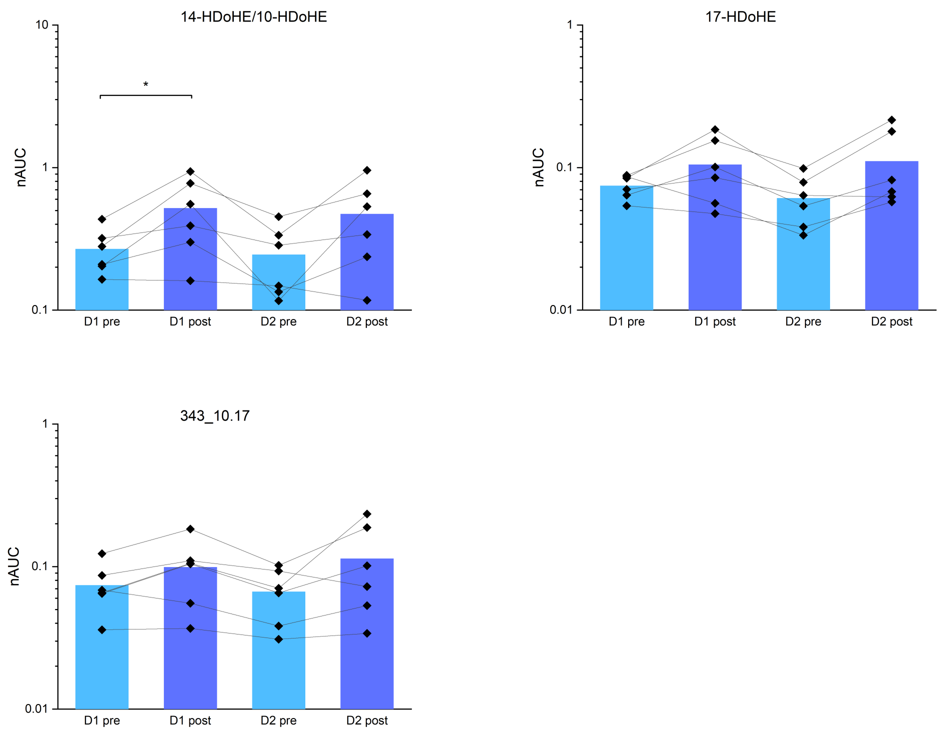

Figure 10: The normalised peak areas of identified HDoHEs and the HDoHE isomer 343_10.17 are shown here. 14-HDoHE and 10-HDoHE could not be separated and were quantified together. The samples were taken on two consecutive days before and after photopheresis therapy, with D1 referring to samples taken on the first day and D2 the second day. Data points belonging to the same patient are connected by a line.

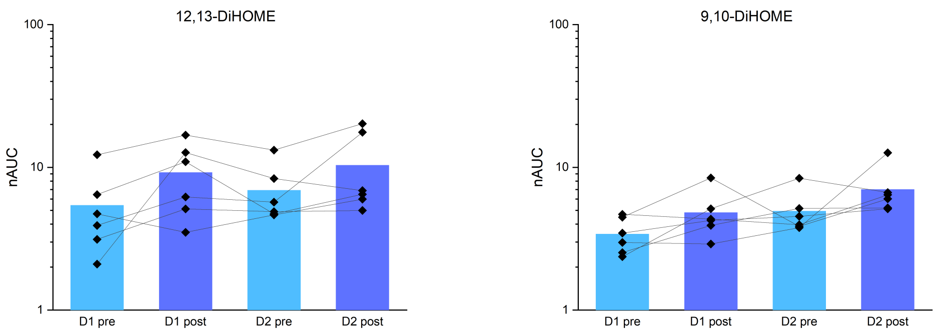

Figure 11: The normalised peak areas of identified DiHOMEs are shown here. The samples were taken on two consecutive days before and after photopheresis therapy, with D1 referring to samples taken on the first day and D2 the second day. Data points belonging to the same patient are connected by a line. A significance of p<0.05 during the paired T-test is marked by an asterisk *.

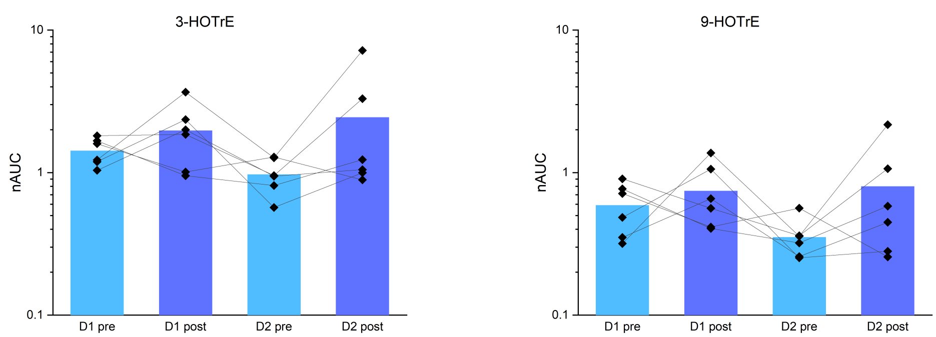

Figure 12: The normalised peak areas of identified HOTrEs are shown here. The samples were taken on two consecutive days before and after photopheresis therapy, with D1 referring to samples taken on the first day and D2 the second day. Data points belonging to the same patient are connected by a line.

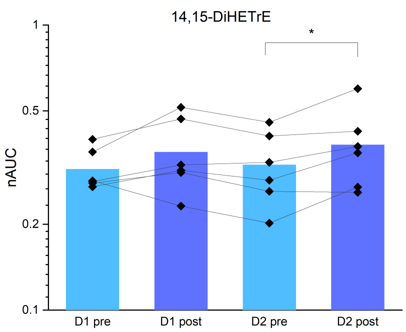

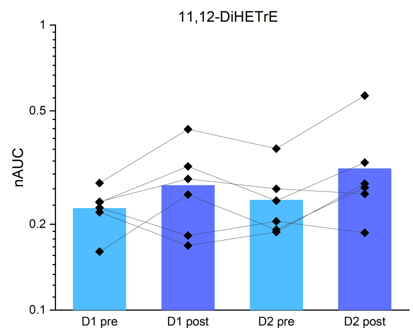

Figure 13: The normalised peak areas of identified DiHETrEs are shown here. The samples were taken on two consecutive days before and after photopheresis therapy, with D1 referring to samples taken on the first day and D2 the second day. Data points belonging to the same patient are connected by a line. A significance of $p<0.05$ during the paired T-test is marked by an asterisk *.

4.2 Method Development

As part of the master's thesis, a UHPLC-MS/MS method based on that described by Lagerborg et al. was partially developed and compared with the original method used for the analysis of the ECP samples [72]. Standard solutions were prepared at concentrations from 1 ng/mL to 500 ng/mL and measured with both the original method and the developed method. The results were then compared with each other.

The main advantage of the developed method is the runtime of 9.5 min compared to the original method's 20 min, which would allow for a higher sample throughput. In addition, the developed method does not use the toxic MeOH as a component of the mobile phase, unlike the original method.

During the first series of measurements of the developed method, which used a Top 2 DDA method, there were only around 6 data points for each chromatographic peak in the extracted ion chromatogram, which was insufficient for accurate quantification. The coefficients of variation (CVs), which is the standard deviation divided by the average and converted to percentage, of the individual deuterated standards ranged between 4.8-9.5%, compared to 1.6-2.3% in the original method. (Table 7)

After switching from the previous Top 2 DDA method to a Top 1 DDA method, the scan rate was almost doubled. The measured peaks had thus more data points, around 15-20, and could be quantified more accurately. The CV of the internal standards was reduced to around 2.0-4.3%. While this was still higher than in the original method, there was a large improvement over the Top 2 DDA method. Further data analysis was thus carried out using the results from the Top 1 DDA method. The untargeted Top 1 DDA method would result in fewer MS2 spectra than the Top 2 DDA method, which may affect the identification of analytes in a sample.

29 analytes were measured at different concentrations with both the original and the developed method. A summary of the results, including the lowest concentration where the standard could still be quantified, are shown in Table 6.

Linear fitting was performed with OriginPro to generate a calibration curve for each of the standards, whereby the intercept was set to 0. An example of such a linear fit can be seen in Figure 15. The standards 13S-HpODE, 14,15-DiHETrE, 11,12-DiHETrE, 8,9-DiHETrE and 5,6-DiHETrE did not have enough data points to generate a calibration curve. (Table 8)

A number of standards, such as many of the HDoHEs and the HODEs,

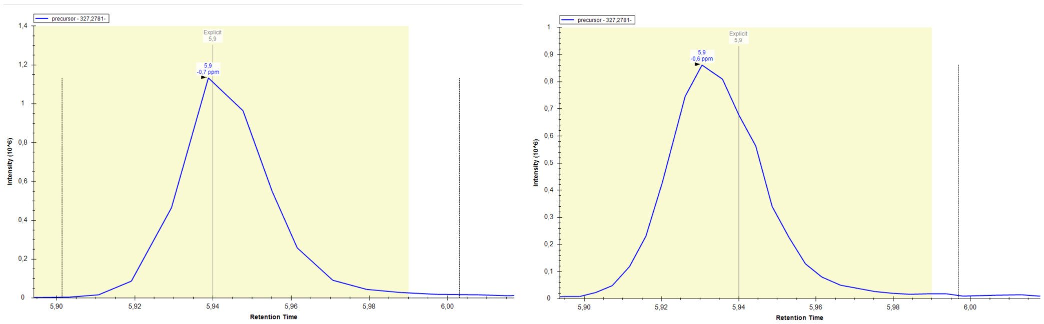

(a) Developed Method Top2 (b) Developed Method Top1

Figure 14: Comparison of the deuterated standard 15S-HETE-d8 during method development measured with a DDA Top 2 method (a) and a DDA Top 1 method (b). The peak obtained with the DDA Top 2 method peak consists of 7 data points, which is too low for an accurate determination of peak area, while peak obtained with the DDA Top 1 method consists of 15-20 data points.

appeared to be quantifiable at lower concentrations using the developed method compared to the original method. 5-HEPE, 12-epi-LTB4 and 13S-HpODE were the only standards where the lowest quantifiable concentration was greater in the developed method than the original method. (Table 6)

As only one series of measurement was carried out for both the original method and the method under development, it was not possible to calculate and compare the LOD and LOQ of the different methods. That would require calculating the standard deviation based on multiple measurements, from which the LOD and LOQ can be calculated as 3x and 10x of the standard deviation [77]. Further measurements of the standards are planned to obtain their LOD and LOQ.

Additional work is still required to fully develop the new method. The gradient or mobile phase could be adjusted to better separate closely eluting oxylipins such as 8-HEPE and 12-HEPE. The LOQ and LOD of standards in the new method should also be determined and compared with the original method. Pairing the method with an ion mobility spectrometer was also under consideration. However, further development of this method is not part of the master's thesis and will be carried out by others.

Table 6: m/z and MS2 product ions of the standards used during method development are shown here. The retention time (RT) as well as the lowest concentration (Lowest c) where the standard could still be quantified were compared between the original method and the developed method.

Molecule	m/z	MS2 product ion	Original Method		Developed Method	
			RT	Lowest c (ng/mL)	RT	Lowest c (ng/mL)
20-HETE	319	289	9.71	5	5.65	5
11S-HETE	319	167	10.48	1	6.05	1
9S-HETE	319	167	10.73	1	6.12	1
8S-HETE	319	155	10.62	5	6.09	1
13R-HODE	295	193	10.13	5	5.92	1
9R-HODE	295	171	10.15	5	5.96	1
13-HDoHE	343	193	10.41	5	6.00	5
7-HDoHE	343	281	10.65	5	6.08	1
17-HDoHE	343	263	10.36	30	5.97	5
8-HDoHE	343	189	10.72	30	6.10	5
10-HDoHE	343	153	10.49	5	6.04	1
20-HDoHE	343	153	10.50	5	6.04	5
11-HDoHE	343	121	10.60	5	6.07	1
4-HDoHE	343	101	10.99	5	6.17	1
18-HEPE	317	255	9.48	5	5.41	5
8-HEPE	317	155	9.79	5	5.68	5
9-HEPE	317	207	9.90	5	5.74	5
5-HEPE	317	115	10.01	5	5.83	10
12-HEPE	317	179	9.86	5	5.69	5
13-Oxo-ODE	293	-	10.47	5	5.94	1
12-epi-LTB4	335	195	8.13	10	4.65	30
5-Oxo-ETE	317	203	11.36	5	6.20	1
5(S)-HETrE	321	115	11.69	5	6.30	1
6-trans-LTB4	335	173	7.95	5	4.54	5
14,15-DiHETrE	337	207	8.89	50	5.12	50
11,12-DiHETrE	337	167	9.18	50	5.32	50
8,9-DiHETrE	337	127	9.40	50	5.49	50
5,6-DiHETrE	337	145	9.70	50	5.74	50
13S-HpODE	311	293	10.29	100	6.00	500
15S-HETE-d8	327	223	10.25	-	5.94	-
12SHETE-d8	327	184	10.57	-	6.07	-
5S-HETE-d8	327	116	10.77	-	6.14	-
5-Oxo-ETE-d7	324	280	11.31	-	6.19	-
PGE2-d4	355	275	5.65	-	2.87	-
20-HETE-d6	325	281	9.69	-	5.62	-
14,15-DiHETrE-d11	348	207	8.84	-	5.08	-
11,12-DiHETrE-d11	348	167	9.13	-	5.28	-
8-isoPGf2alpha-d4	357	313	4.80	-	2.26	-

Table 7: CV of deuterated standards during method development. The developed method Top2 used a Top 2 DDA method while developed method Top1 used a Top 1 DDA method.

Deuterated Standard	CV [%]		
	Original Method	Developed Method Top2	Developed Method Top1
15S-HETE-d8	2.2	7.5	3.0
12SHETE-d8	2.3	8.4	3.3
5S-HETE-d8	1.6	9.5	4.3
5-Oxo-ETE-d7	2.0	6.2	2.1
PGE2-d4	1.9	4.8	2.5
20-HETE-d6	2.0	5.9	2.5
14,15-DiHETrE-d11	1.6	8.5	3.9
11,12-DiHETrE-d11	2.1	6.7	2.0
8-isoPGf2alpha-d4	1.9	6.6	2.3

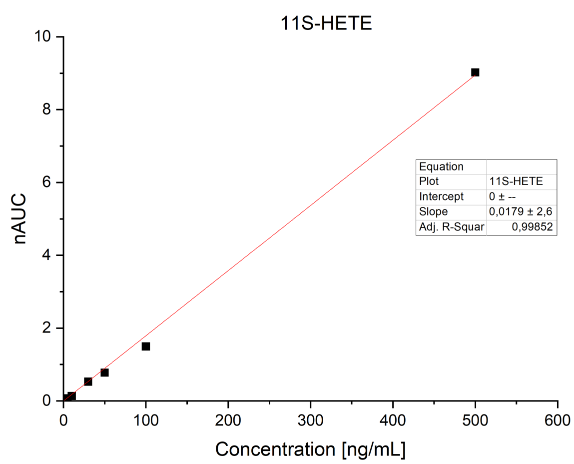

Figure 15: Example of a linear fit of 11S-HETE performed during method development.

Table 8: Linear fitting of the nAUC against the concentration [ng/mL] was performed with an intercept of 0. The calculated slope and the adjusted R^2 are shown here in this table. The standards 13S-HpODE, 14,15-DiHETrE, 11,12-DiHETrE, 8,9-DiHETrE and 5,6-DiHETrE did not have enough data points for linear fitting and are not shown here.

	Original Method		Developed Method	
	Slope	Adj. R^2	Slope	Adj. R^2
20-HETE	5.55E-03	0.9988	3.78E-03	0.9982
11S-HETE	1.79E-02	0.9985	7.17E-03	0.9993
9S-HETE	2.09E-02	0.9975	6.79E-03	0.9991
8S-HETE	9.05E-03	0.9990	5.14E-03	0.9979
13R-HODE	1.07E-02	0.9993	4.64E-03	0.9994
9R-HODE	5.82E-03	0.9965	2.08E-03	0.9982
13-HDoDE	5.56E-03	0.9992	3.04E-03	0.9993
7-HDoDE	1.15E-02	0.9982	5.32E-03	0.9989
17-HDoHE	2.44E-03	0.9950	1.45E-03	0.9967
8-HDoHE	4.16E-03	0.9930	1.91E-03	0.9907
10-HDoHE	6.92E-03	0.9987	3.49E-03	0.9985
20-HDoHE	5.13E-03	0.9990	5.01E-03	0.9988
11-HDoHE	8.77E-03	0.9988	5.20E-03	0.9983
4-HDoHE	7.83E-03	0.9996	3.93E-03	0.9986
18-HEPE	4.48E-03	0.9986	2.87E-03	0.9977
8-HEPE	3.25E-03	0.9979	2.61E-03	0.9990
9-HEPE	3.90E-03	0.9977	2.51E-03	0.9992
5-HEPE	2.23E-03	0.9972	2.05E-03	0.9993
12-HEPE	6.62E-03	0.9998	7.42E-03	0.9966
13-Oxo-ODE	1.05E-02	0.9982	1.51E-03	0.9981
12-epi-LTB4	8.10E-04	0.9963	2.33E-03	0.9943
5-Oxo-ETE	2.27E-02	0.9999	8.52E-03	0.9950
5(S)-HETrE	1.69E-02	0.9998	6.42E-03	0.9947
6-trans-LTB4	4.60E-03	0.9988	1.07E-02	0.9950

5 Summary

Extracorporeal photopheresis is a procedure where the buffy coat from a patient is obtained, exposed to UVA radiation before being returned to the patient. It was introduced as a therapy for the autoimmune disease CTCL since 1988, and is also being considered as a possible therapy for other autoimmune diseases. How ECP influences the immune system and achieves its therapeutic effects is not well understood. Activation of DCs or phagocytosis of apoptotic lymphocytes have been proposed as possible mechanisms.

An important class of signal molecules for the immune system is the oxylipins. These oxygenated metabolites of PUFAs, which includes eicosanoids such as prostaglandins, play a vital role in the initiation and resolution of inflammation. They are primarily generated by the enzymatic COX, LOX and CYP450 pathways. By analysing the oxylipin profiles of patients undergoing ECP, more information how this therapy influences the immune system may be discovered.

For this master's thesis, plasma samples from six patients were received from the Vienna General Hospital which were taken during two consecutive days of ECP, both before and after ECP on each day. Oxylipins and PUFAs were extracted via SPE and analysed with an UHPLC-MS/MS method.

A total of 32 molecules, which included oxylipins, PUFAs as well as unknown isomers and isobars, were chosen for statistical analysis. The relative nAUC levels of these analytes to the deuterated internal standards was calculated, and a paired T-test comparing the samples before and after each day's ECP was performed.

The PUFAs and their isomers appear to have a larger fold change in general than the oxylipins. Among the PUFAs and their isomers, the analyte labeled 277_12.47 had the greatest fold change, with AA, AA_12.91, LA and 275_12.14 having the least. Among the oxylipins and their isomers, 12-HEPE/8-HEPE and 14-HDoHE/10-HDoHE had the greatest increase in the samples post treatment compared to pre-treatment. The levels of most analytes before ECP were similar on both days, implying that the effects of ECP on the oxylipin profile is short-lived.

On the first day 277_12.38, 12-HEPE/8-HEPE, 12S-HETE/8S-HETE, 11-HEPE and 14-HDoHE/10-HDoHE were significantly increased after ECP, while on the second day 277_12.38, 12-HEPE/8-HEPE, AA_12.91, DHA, 277_12.47, 275_12.14, 15S-HETE, 11S-HETE, 5S-HETE and 14,15-DiHETrE were significantly increased. Only 277_12.38 and 12-HEPE/8-HEPE were significantly increased on both days. These results are likely due to the small sample size of six patients, limiting the statistical analysis. Furthermore, the patients had differing health conditions and the medication taken by the patients was also very heterogenous. Future studies should both have a larger sample size as well as a more homogenous patient background.

In addition to the oxylipin analysis of plasma samples from patients undergoing ECP, a new UPHLC-MS/MS method based on an example from literature was partially developed and compared to the former method. The new UHPLC method utilises a smaller column and has a shorter runtime, which would allow for a higher sample throughput. Standard solutions were prepared at different concentrations and measured with both methods. Initial measurements of standard solutions have shown promising results, though it was neccessary to change the mass spectrometer settings from a DDA Top 2 method to a DDA Top 1 method to obtain satisfactory chromatographic peaks. Further development of the method would continue to be carried out by others in order to better optimise the separation of analytes. Eventually, the UHPLC method may be coupled to a TimsTOF mass spectrometer, which combines an ion mobility spectrometer and a time-of-flight mass spectrometer to obtain more information about the analytes.

6 Abstract/Zusammenfassung

Abstract

Extracorporeal photopheresis is a treatment for CTCL that has been present for decades. However, the mechanisms behind it's therapeutic effects are still not well understood, although there are theories that it is due to the activation of DCs or the phagocytosis of apoptotic lymphocytes.

In this master's thesis, the oxylipin profiles of plasma samples from six patients undergoing ECP therapy over the course of two days were analysed. These molecules are known to play a vital role as lipid mediators in immune response and may provide some information on the effects of ECP on the immune system. After SPE and UHPLC-MS/MS analysis, 32 peaks belonging to oxylipins, their PUFA precursors as well as unknown isomers and isobars were chosen and quantified. The analytes which were significantly increased after ECP therapy were different on the two different days. This may be in part due to the small sample size, limiting the statistical analysis.

Of the identified analytes, the PUFA precursors and 12-HEPE/8-HEPE had the largest fold change in samples post-treatment compared to pre-treatment. On the second day, most of the analytes in the pre-treatment samples had returned back to levels similar to the pre-treatment samples of the first day, implying that the effects of ECP on the oxylipin profile in plasma is short-lived.

A new UHPLC-MS/MS method for the analysis of oxylipins was also partially developed as part of the master's thesis with a shorter runtime compared to the established method used for oxylipin analysis of the ECP plasma samples. Initial measurements of standard solutions have shown promising results. Further studies will eventually be carried out in the group based on the results of the thesis.

Zusammenfassung

Extrakorporale Photopherese ist eine Behandlung, die seit Jahrzehnten bei CTCL eingesetzt wird. Die Mechanismen dahinter konnten jedoch noch nicht vollständig erklärt werden. Es gibt Theorien, dass die therapeutische Wirkungen durch das Aktivieren von DCs oder die Phagozytose der apoptotischen Lymphozyten erzeugt wird.

In dieser Masterarbeit werden die Oxylipin-Profile in den Plasmaproben von sechs Patienten, die mit ECP behandelt werden, im Verlauf von zwei Tagen untersucht. Diese Molekülen erfüllen eine wichtige Rolle als Lipidmediatoren in der Immunantwort, und könnten möglicherweise im Verlauf der ECP-Behandlung das Immunsystem beeinflussen. Nach SPE und UHPLC-MS/MS wurden 32 Peaks gewählt und quantifiziert, die zu den Oxylipinen, ihren PUFA-Precursors und deren Isomeren und Isobaren gehören. An den zwei Tagen wurden unterschiedliche Analyten nach der ECP-Behandlung signifikant erhöht. Dies ist wahrscheinlich auf die kleine Probeanzahl zurückzuführen, welche die statistische Analyse beschränkt.

Die PUFA-Precursors und 12-HEPE/8-HEPE hatten die größten Fold-Changes in den Proben nach der Behandlung im Vergleich zu den Proben vor der Behandlung. Am zweiten Tag vor der Behandlung waren die meisten Analyten in den Proben auf Levels zurückgekehrt, die am ersten Tag in den Proben vor der Behandlung ähnlich waren. Dies deutet auf eine kurzfristige Wirkung von ECP auf das Oxylipin-Profil im Plasma.

Als Teil der Masterarbeit wurde auch eine UHPLC-MS/MS Methodenentwicklung teilweise durchgeführt. Die neue Methode soll eine kürzere Laufzeit im Vergleich zu der etablierten Methode der Oxylipin-Analyse der ECP Plasmaproben haben. Die ersten Messungen der Standardlösungen haben vielversprechende Ergebnisse geliefert. Basierend auf die Resultate der Arbeit, werden in der Abteilung eventuell weiterführende Studien durchgeführt.

References

[1] Lydic TA, Goo YH. Lipidomics unveils the complexity of the lipidome in metabolic diseases. Clin Transl Med. 2018 Jan 26;7(1):4. doi: 10.1186/s40169-018-0182-9. PMID: 29374337; PMCID: PMC5786598.

[2] Quehenberger O, Armando AM, Brown AH, et al. Lipidomics reveals a remarkable diversity of lipids in human plasma. J Lipid Res. 2010;51(11):3299-3305. doi:10.1194/jlr.M009449

[3] Turk HF, Chapkin RS. Membrane lipid raft organization is uniquely modified by n-3 polyunsaturated fatty acids. Prostaglandins Leukot Essent Fatty Acids. 2013 Jan;88(1):43-7. doi: 10.1016/j.plefa.2012.03.008. Epub 2012 Apr 18. PMID: 22515942; PMCID: PMC3404206.

[4] Leng X, Kinnun JJ, Cavazos AT, et al. All n-3 PUFA are not the same: MD simulations reveal differences in membrane organization for EPA, DHA and DPA. Biochim Biophys Acta Biomembr. 2018;1860(5):1125-1134. doi:10.1016/j.bbamem.2018.01.002

[5] T. Yuzyuk, B. Lozier, E.L. Schwarz, K. Viau, E. Kish-Trier, I. De Biase, Intra-individual variability of long-chain fatty acids (C12–C24) in plasma and red blood cells, Prostaglandins, Leukotrienes and Essential Fatty Acids, Volume 135, 2018, Pages 30-38, ISSN 0952-3278, https://doi.org/10.1016/j.plefa.2018.06.006.

[6] William W. Christie, John L. Harwood; Oxidation of polyunsaturated fatty acids to produce lipid mediators. Essays Biochem 23 September 2020; 64 (3): 401–421. doi: https://doi.org/10.1042/EBC20190082

[7] Hanna VS, Hafez EAA. Synopsis of arachidonic acid metabolism: A review. J Adv Res. 2018 Mar 13;11:23-32. doi: 10.1016/j.jare.2018.03.005. PMID: 30034873; PMCID: PMC6052663.

[8] Gabbs M, Leng S, Devassy JG, Monirujjaman M, Aukema HM. Advances in Our Understanding of Oxylipins Derived from Dietary PUFAs. Adv Nutr. 2015 Sep 15;6(5):513-40. doi: 10.3945/an.114.007732. PMID: 26374175; PMCID: PMC4561827.

[9] Kulterer OC, Niederstaetter L, Herz CT, et al. The Presence of Active Brown Adipose Tissue Determines Cold-Induced Energy

Expenditure and Oxylipin Profiles in Humans. J Clin Endocrinol Metab. 2020;105(7):dgaa183. doi:10.1210/clinem/dgaa183

[10] Sala, A., Folco, G., Murphy, R. C. (2010). Transcellular biosynthesis of eicosanoids. Pharmacological reports : PR, 62(3), 503–510. https://doi.org/10.1016/s1734-1140(10)70306-6

[11] Rouzer, C. A., Marnett, L. J. (2009). Cyclooxygenases: structural and functional insights. Journal of lipid research, 50 Suppl(Suppl), S29–S34. https://doi.org/10.1194/jlr.R800042-JLR200

[12] Dennis, E., Norris, P. Eicosanoid storm in infection and inflammation. Nat Rev Immunol 15, 511–523 (2015). https://doi.org/10.1038/nri3859

[13] Serhan C. N. (2014). Pro-resolving lipid mediators are leads for resolution physiology. Nature, 510(7503), 92–101. https://doi.org/10.1038/nature13479

[14] Musiek ES, Yin H, Milne GL, Morrow JD. Recent advances in the biochemistry and clinical relevance of the isoprostane pathway. Lipids. 2005 Oct;40(10):987-94. doi: 10.1007/s11745-005-1460-7. PMID: 16382569.

[15] Galano JM, Lee JC, Gladine C, et al. Non-enzymatic cyclic oxygenated metabolites of adrenic, docosahexaenoic, eicosapentaenoic and α-linolenic acids; bioactivities and potential use as biomarkers. Biochim Biophys Acta. 2015;1851(4):446-455. doi:10.1016/j.bbalip.2014.11.004

[16] Tejero J, Kapralov AA, Baumgartner MP, et al. Peroxidase activation of cytoglobin by anionic phospholipids: Mechanisms and consequences. Biochim Biophys Acta. 2016;1861(5):391-401. doi:10.1016/j.bbalip.2016.02.022

[17] Tyurina YY, St Croix CM, Watkins SC, et al. Redox (phospho)lipidomics of signaling in inflammation and programmed cell death. J Leukoc Biol. 2019;106(1):57-81. doi:10.1002/JLB.3MIR0119-004RR

[18] Kulkarni A, Nadler JL, Mirmira RG, Casimiro I. Regulation of Tissue Inflammation by 12-Lipoxygenases. Biomolecules. 2021;11(5):717. Published 2021 May 11. doi:10.3390/biom11050717

[19] Du Y, Taylor CG, Aukema HM, Zahradka P. Role of oxylipins generated from dietary PUFAs in the modulation of endothelial cell function. Prostaglandins Leukot Essent Fatty Acids. 2020 Sep;160:102160. doi: 10.1016/j.plefa.2020.102160. Epub 2020 Jul 19. PMID: 32717531.

[20] Tahir A, Bileck A, Muqaku B, et al. Combined Proteome and Eicosanoid Profiling Approach for Revealing Implications of Human Fibroblasts in Chronic Inflammation. Anal Chem. 2017;89(3):1945-1954. doi:10.1021/acs.analchem.6b04433

[21] Maseda D, Ricciotti E, Crofford LJ. Prostaglandin regulation of T cell biology. Pharmacol Res. 2019 Nov;149:104456. doi: 10.1016/j.phrs.2019.104456. Epub 2019 Sep 22. PMID: 31553935.

[22] English K, Ryan JM, Tobin L, Murphy MJ, Barry FP, Mahon BP. Cell contact, prostaglandin E(2) and transforming growth factor beta 1 play non-redundant roles in human mesenchymal stem cell induction of CD4+CD25(High) forkhead box P3+ regulatory T cells. Clin Exp Immunol. 2009;156(1):149-160. doi:10.1111/j.1365-2249.2009.03874.x

[23] Freire, M. O., Van Dyke, T. E. (2013). Natural resolution of inflammation. Periodontology 2000, 63(1), 149–164. https://doi.org/10.1111/prd.12034

[24] de Bus I, Witkamp R, Zuilhof H, Albada B, Balvers M. The role of n-3 PUFA-derived fatty acid derivatives and their oxygenated metabolites in the modulation of inflammation. Prostaglandins Other Lipid Mediat. 2019 Oct;144:106351. doi: 10.1016/j.prostaglandins.2019.106351. Epub 2019 Jun 28. PMID: 31260750.

[25] Cas MD, Roda G, Li F, Secundo F. Functional Lipids in Autoimmune Inflammatory Diseases. Int J Mol Sci. 2020 Apr 27;21(9):3074. doi: 10.3390/ijMS21093074. PMID: 32349258; PMCID: PMC7246500.

[26] Johnson AM, Kleczko EK, Nemenoff RA. Eicosanoids in Cancer: New Roles in Immunoregulation. Front Pharmacol. 2020 Nov 18;11:595498. doi: 10.3389/fphar.2020.595498. PMID: 33364964; PMCID: PMC7751756.

[27] Greene ER, Huang S, Serhan CN, Panigrahy D. Regulation of inflammation in cancer by eicosanoids. Prostaglandins Other Lipid Mediat. 2011;96(1-4):27-36. doi:10.1016/j.prostaglandins.2011.08.004

[28] Noonan DM, De Lerma Barbaro A, Vannini N, Mortara L, Albini A. Inflammation, inflammatory cells and angiogenesis: decisions and indecisions. Cancer Metastasis Rev. 2008;27(1):31-40. doi:10.1007/s10555-007-9108-5

[29] Chocholoušková M, Jirásko R, Vrána D, Gatěk J, Melichar B, Holčapek M. Reversed phase UHPLC/ESI-MS determination of oxylipins in human plasma: a case study of female breast cancer. Anal Bioanal Chem. 2019 Feb;411(6):1239-1251. doi: 10.1007/s00216-018-1556-y. Epub 2019 Jan 8. PMID: 30617406.

[30] Muqaku B, Eisinger M, Meier SM, et al. Multi-omics Analysis of Serum Samples Demonstrates Reprogramming of Organ Functions Via Systemic Calcium Mobilization and Platelet Activation in Metastatic Melanoma. Mol Cell Proteomics. 2017;16(1):86-99. doi:10.1074/mcp.M116.063313

[31] Evangelista EA, Cho CW, Aliwarga T, Totah RA. Expression and Function of Eicosanoid-Producing Cytochrome P450 Enzymes in Solid Tumors. Front Pharmacol. 2020 Jun 9;11:828. doi: 10.3389/fphar.2020.00828. PMID: 32581794; PMCID: PMC7295938.

[32] Chaplin DD. Overview of the immune response. J Allergy Clin Immunol. 2010;125(2 Suppl 2):S3-S23. doi:10.1016/j.jaci.2009.12.980

[33] Ostermann AI, Koch E, Rund KM, Kutzner L, Mainka M, Schebb NH. Targeting esterified oxylipins by LC-MS - Effect of sample preparation on oxylipin pattern. Prostaglandins Other Lipid Mediat. 2020 Feb;146:106384. doi: 10.1016/j.prostaglandins.2019.106384. Epub 2019 Nov 4. PMID: 31698140.

[34] Ostermann AI, Willenberg I, Schebb NH. Comparison of sample preparation methods for the quantitative analysis of eicosanoids and other oxylipins in plasma by means of LC-MS/MS. Anal Bioanal Chem. 2015 Feb;407(5):1403-14. doi: 10.1007/s00216-014-8377-4. Epub 2014 Dec 27. PMID: 25542569.

[35] Liakh I, Pakiet A, Sledzinski T, Mika A. Modern Methods of Sample Preparation for the Analysis of Oxylipins in Biological Samples. Molecules. 2019 Apr 25;24(8):1639. doi: 10.3390/molecules24081639. PMID: 31027298; PMCID: PMC6515351.

[36] Mohri M, Rezapoor H. Effects of heparin, citrate, and EDTA on plasma biochemistry of sheep: comparison with serum. Res Vet Sci. 2009;86(1):111-114. doi:10.1016/j.rvsc.2008.05.010

[37] Astarita G, Kendall AC, Dennis EA, Nicolaou A. Targeted lipidomic strategies for oxygenated metabolites of polyunsaturated fatty acids. Biochim Biophys Acta. 2015;1851(4):456-468. doi:10.1016/j.bbalip.2014.11.012

[38] Tsikas D, Zoerner AA. Analysis of eicosanoids by LC-MS/MS and GC-MS/MS: a historical retrospect and a discussion. J Chromatogr B Analyt Technol Biomed Life Sci. 2014 Aug 1;964:79-88. doi: 10.1016/j.jchromb.2014.03.017. Epub 2014 Mar 21. PMID: 24742369.

[39] Chhonker YS, Bala V, Murry DJ. Quantification of eicosanoids and their metabolites in biological matrices: a review. Bioanalysis. 2018 Dec;10(24):2027-2046. doi: 10.4155/bio-2018-0173. Epub 2018 Nov 6. PMID: 30412686; PMCID: PMC6562698.

[40] Liakh I, Pakiet A, Sledzinski T, Mika A. Methods of the Analysis of Oxylipins in Biological Samples. Molecules. 2020 Jan 15;25(2):349. doi: 10.3390/molecules25020349. PMID: 31952163; PMCID: PMC7024226.

[41] Watrous JD, Niiranen TJ, Lagerborg KA, Henglin M, Xu YJ, Rong J, Sharma S, Vasan RS, Larson MG, Armando A, Mora S, Quehenberger O, Dennis EA, Cheng S, Jain M. Directed Non-targeted Mass Spectrometry and Chemical Networking for Discovery of Eicosanoids and Related Oxylipins. Cell Chem Biol. 2019 Mar 21;26(3):433-442.e4. doi: 10.1016/j.chembiol.2018.11.015. Epub 2019 Jan 17. PMID: 30661990; PMCID: PMC6636917.

[42] Hellhake S, Meckelmann SW, Empl MT, Rentmeister K, Wißdorf W, Steinberg P, Schmitz OJ, Benter T, Schebb NH. Non-targeted and targeted analysis of oxylipins in combination with charge-switch derivatization by ion mobility high-resolution mass spectrometry. Anal

Bioanal Chem. 2020 Sep;412(23):5743-5757. doi: 10.1007/s00216-020-02795-2. Epub 2020 Jul 22. PMID: 32699965; PMCID: PMC7413910.

[43] Kyle JE, Aly N, Zheng X, Burnum-Johnson KE, Smith RD, Baker ES. Evaluating lipid mediator structural complexity using ion mobility spectrometry combined with mass spectrometry. Bioanalysis. 2018;10(5):279-289. doi:10.4155/bio-2017-0245

[44] Gabelica V, Shvartsburg AA, Afonso C, et al. Recommendations for reporting ion mobility Mass Spectrometry measurements. Mass Spectrom Rev. 2019;38(3):291-320. doi:10.1002/mas.21585

[45] Dasilva G, Muñoz S, Lois S, Medina I. Non-Targeted LC-MS/MS Assay for Screening Over 100 Lipid Mediators from ARA, EPA, and DHA in Biological Samples Based on Mass Spectral Fragmentations. Molecules. 2019 Jun 19;24(12):2276. doi: 10.3390/molecules24122276. PMID: 31248084; PMCID: PMC6630234.

[46] Rhishikesh Thakare, Yashpal S. Chhonker, Nagsen Gautam, Jawaher Abdullah Alamoudi, Yazen Alnouti, Quantitative analysis of endogenous compounds, Journal of Pharmaceutical and Biomedical Analysis, Volume 128, 2016, Pages 426-437, ISSN 0731-7085, https://doi.org/10.1016/j.jpba.2016.06.017.

[47] Rund KM , Nolte F , Doricic J , Greite R , Schott S , Lichtinghagen R , Gueler F , Schebb NH . Clinical blood sampling for oxylipin analysis - effect of storage and pneumatic tube transport of blood on free and total oxylipin profile in human plasma and serum. Analyst. 2020 Mar 21;145(6):2378-2388. doi: 10.1039/c9an01880h. Epub 2020 Feb 10. PMID: 32037406.

[48] Wójcik P, Gegotek A, Žarković N, Skrzydlewska E. Oxidative Stress and Lipid Mediators Modulate Immune Cell Functions in Autoimmune Diseases. Int J Mol Sci. 2021 Jan 13;22(2):723. doi: 10.3390/ijMS22020723. PMID: 33450863; PMCID: PMC7828321.

[49] Cho A, Jantschitsch C, Knobler R. Extracorporeal Photopheresis-An Overview. Front Med (Lausanne). 2018 Aug 27;5:236. doi: 10.3389/fmed.2018.00236. PMID: 30211164; PMCID: PMC6119964.

[50] Pulitzer M. Cutaneous T-cell Lymphoma. Clin Lab Med. 2017;37(3):527-546. doi:10.1016/j.cll.2017.06.006

[51] Helmberg W, Sipurzynski S, Groselje-Strehle A, Greinix H, Schlenke P. Does Offline Beat Inline Treatment: Investigation into Extracorporeal Photopheresis. Transfus Med Hemother. 2020;47(3):198-204. doi:10.1159/000506750

[52] Arora S, Setia R. Extracorporeal photopheresis: Review of technical aspects. Asian J Transfus Sci 2017;11:81-6

[53] Wei BM, Hanlon D, Khalil D, Han P, Tatsuno K, Sobolev O, Edelson RL. Extracorporeal Photochemotherapy: Mechanistic Insights Driving Recent Advances and Future Directions. Yale J Biol Med. 2020 Mar 27;93(1):145-159. PMID: 32226344; PMCID: PMC7087063.

[54] Diekmann J, Theves I, Thom KA, Gilch P. Tracing the Photoaddition of Pharmaceutical Psoralens to DNA. Molecules. 2020;25(22):5242. Published 2020 Nov 10. doi:10.3390/molecules25225242

[55] Reinheckel T, Bohne M, Halangk W, Augustin W, Gollnick H. Evaluation of UVA-mediated oxidative damage to proteins and lipids in extracorporeal photoimmunotherapy. Photochem Photobiol. 1999 May;69(5):566-70. PMID: 10333762.

[56] Rao, V., Saunes, M., Jørstad, S. and Moen, T. (2008), In Vitro Experiments Demonstrate that Monocytes and Dendritic Cells are Rendered Apoptotic by Extracorporeal Photochemotherapy, but Exhibit Unaffected Surviving and Maturing Capacity after 30 Gy Gamma Irradiation. Scandinavian Journal of Immunology, 68: 645-651. https://doi.org/10.1111/j.1365-3083.2008.02179.x

[57] Budde H, Berntsch U, Riggert J, Legler TJ. In vitro effects of different 8-methoxypsoralen treatment protocols for extracorporeal photopheresis on mononuclear cells. Cent Eur J Immunol. 2017;42(1):1-9. doi:10.5114/ceji.2017.67312

[58] Fadok VA, Bratton DL, Konowal A, Freed PW, Westcott JY, Henson PM. Macrophages that have ingested apoptotic cells in vitro inhibit proinflammatory cytokine production through autocrine/paracrine

mechanisms involving TGF-beta, PGE2, and PAF. J Clin Invest. 1998 Feb 15;101(4):890-8. doi: 10.1172/JCI1112. PMID: 9466984; PMCID: PMC508637.

[59] Szczepiorkowski ZM, Burnett CA, Dumont LJ, Abhyankar SH. Apheresis buffy coat collection without photoactivation has no effect on apoptosis, cell proliferation, and total viability of mononuclear cells collected using photopheresis systems. Transfusion. 2018 Apr;58(4):943-950. doi: 10.1111/trf.14532. Epub 2018 Feb 16. PMID: 29451308.

[60] Arita K, Yamamoto Y, Takehara Y, Utsumi T, Kanno T, Miyaguchi C, Akiyama J, Yoshioka T, Utsumi K. Mechanisms of enhanced apoptosis in HL-60 cells by UV-irradiated n-3 and n-6 polyunsaturated fatty acids. Free Radic Biol Med. 2003 Jul 15;35(2):189-99. doi: 10.1016/s0891-5849(03)00310-1. PMID: 12853075.

[61] Wiswedel I, Bohne M, Hirsch D, Kühn H, Augustin W, Gollnick H. A sensitive gas chromatography-mass spectrometry assay reveals increased levels of monohydroxyeicosatetraenoic acid isomers in human plasma after extracorporeal photoimmunotherapy and under in vitro ultraviolet A exposure. J Invest Dermatol. 2000 Sep;115(3):499-503. doi: 10.1046/j.1523-1747.2000.00053.x. PMID: 10951289.

[62] Kuzmina Z, Stroncek D, Pavletic SZ. Extracorporeal photopheresis as a therapy for autoimmune diseases. J Clin Apher. 2015;30(4):224-237. doi:10.1002/jca.21367

[63] Peter Szodoray, Gabor Papp, Britt Nakken, Mariann Harangi, Margit Zeher, The molecular and clinical rationale of extracorporeal photochemotherapy in autoimmune diseases, malignancies and transplantation, Autoimmunity Reviews, Volume 9, Issue 6, 2010, Pages 459-464, ISSN 1568-9972, https://doi.org/10.1016/j.autrev.2009.12.011.

[64] Ardrey, Robert E. (2003). Liquid Chromatography (1. Aufl.). Wiley.

[65] McMaster, M. C. (2005). LC/MS: a practical user's guide. John Wiley.

[66] Nováková L, Vlcková H. A review of current trends and advances in modern bio-analytical methods: chromatography and sample preparation. Anal Chim Acta. 2009;656(1-2):8-35. doi:10.1016/j.aca.2009.10.004

[67] Zhou J, Yin Y. Strategies for large-scale targeted metabolomics quantification by liquid chromatography-mass spectrometry. Analyst. 2016;141(23):6362-6373. doi:10.1039/c6an01753c

[68] Vidova V, Spacil Z. A review on mass spectrometry-based quantitative proteomics: Targeted and data independent acquisition. Anal Chim Acta. 2017;964:7-23. doi:10.1016/j.aca.2017.01.059

[69] Zubarev RA, Makarov A. Orbitrap mass spectrometry. Anal Chem. 2013;85(11):5288-5296. doi:10.1021/ac4001223

[70] Eliuk S, Makarov A. Evolution of Orbitrap Mass Spectrometry Instrumentation. Annu Rev Anal Chem (Palo Alto Calif). 2015;8:61-80. doi:10.1146/annurev-anchem-071114-040325

[71] Scheltema RA, Hauschild JP, Lange O, et al. The Q Exactive HF, a Benchtop mass spectrometer with a pre-filter, high-performance quadrupole and an ultra-high-field Orbitrap analyzer. Mol Cell Proteomics. 2014;13(12):3698-3708. doi:10.1074/mcp.M114.043489

[72] Lagerborg KA, Watrous JD, Cheng S, Jain M. High-Throughput Measure of Bioactive Lipids Using Non-targeted Mass Spectrometry. Methods Mol Biol. 2019;1862:17-35. doi: 10.1007/978-1-4939-8769-6_2. PMID: 30315457.

[73] LMSD: LIPID MAPS® structure database. Sud M., Fahy E., Cotter D., Brown A., Dennis E., Glass C., Murphy R., Raetz C., Russell D., and Subramaniam S., Nucleic Acids Research 35, D527-32 (2006)

[74] Wishart DS, Feunang YD, Marcu A, et al. HMDB 4.0: the human metabolome database for 2018. Nucleic Acids Res. 2018;46(D1):D608-D617. doi:10.1093/nar/gkx1089

[75] Adams KJ, Pratt B, Bose N, Dubois LG, St John-Williams L, Perrott KM, Ky K, Kapahi P, Sharma V, MacCoss MJ, Moseley MA, Colton CA, MacLean BX, Schilling B, Thompson JW; Alzheimer's Disease Metabolomics Consortium. Skyline for Small Molecules: A Unifying Software Package for Quantitative Metabolomics. J Proteome Res. 2020 Apr 3;19(4):1447-1458. doi: 10.1021/acs.jproteome.9b00640. Epub 2020 Mar 26. PMID: 31984744; PMCID: PMC7127945.

[76] OriginPro, Version 2021. OriginLab Corporation, Northampton, MA, USA

[77] B. Magnusson and U. Örnemark (eds.) Eurachem Guide: The Fitness for Purpose of Analytical Methods – A Laboratory Guide to Method Validation and Related Topics, (2nd ed. 2014). ISBN 978-91-87461-59-0